Aalto-yliopisto
Aalto-universitetet
Aalto University

Master's Programme in Chemical, Biochemical and Materials Engineering

Raw materials in hydrogen direct reduction-electric arc furnace process – simulation and scenario analysis

Kaapo Kopra

Master's thesis
2024

Aalto-yliopisto
Aalto-universitetet
Aalto University

Author Kaapo Kopra

Title of thesis Raw materials in hydrogen direct reduction-electric arc furnace process – simulation and scenario analysis

Programme Chemical, Biochemical and Materials Engineering

Major Sustainable Metals Processing

Thesis supervisor Prof. Daniel Lindberg

Thesis advisor(s) D.Sc. Aleksi Laukka, D.Sc. Marko Kekkonen

Collaborative partner AFRY

Date 28.06.2024 **Number of pages** 80 **Language** English

Abstract

Majority of the steel produced globally is from the blast furnace – basic oxygen furnace process, which accounts for approximately 7-9% of the global carbon dioxide emissions. Consequently, steel producers are shifting towards new processes to reduce their emissions. This study examines the effects of raw materials in hydrogen direct reduction – electric arc furnace process. Which has not been demonstrated utilizing only hydrogen on an industrial scale. The purpose of this thesis is to gain understanding on raw material charges and the criteria for the selection of a suitable charge and by means of modelling examine how different charges effects the process and its product.

The literature review of the thesis introduces current processes in steelmaking and presents the used raw materials for the researched process concept. Additionally, the chemical and thermodynamical basis, as well as the implementation are discussed together with some of the possible challenges that the process concept might face. In the experimental part, the process is modelled by HSC simulation software and the main results of the model are presented and benchmarked to the existing processes. Different scenarios with varying iron ore pellet quality and the charged ratio of scrap and direct reduced iron were simulated with the model. The study examines how raw materials affect, among other things, the produced amount of slag, energy consumption, emissions and the product's purity. The obtained results show that it is beneficial for the process to utilize good-quality iron ore pellets and steel scrap to the extent that it is available, and the product specifications allow it. The HSC software is suitable for a simple mass and energy balance-based process simulation. However, a more rigorous modelling would require data from an industrial scale plant and possibly a more advanced modelling software.

Keywords Steel, Hydrogen direct reduced iron, DRI, Shaft furnace, Electric Arc Furnace, EAF, Modelling, Simulation, HSC

Aalto-yliopisto
Aalto-universitetet
Aalto University

Tekijä Kaapo Kopra

Työn nimi Raaka-ainepanokset vetypohjaisessa kuilu-uuni-valokaariuuniprosessissa – mallinnus ja skenaarioanalyysi

Koulutusohjelma Kemian, bio- ja materiaalitekniikan maisteriohjelma

Pääaine Metallien prosessi- ja kierrätystekniikka

Vastuuopettaja/valvoja Professori Daniel Lindberg

Työn ohjaaja(t) TkT Aleksi Laukka, TkT Marko Kekkonen

Yhteistyötaho AFRY

Päivämäärä 28.06.2024 **Sivumäärä** 80 **Kieli** englanti

Tiivistelmä

Suurin osa maailmassa tuotetusta teräksestä on peräisin masuuni-happikonverteriprosessista, joka aiheuttaa noin 7-9% maapallon hiilidioksidipäästöistä. Tästä johtuen teräksen valmistajat siirtyvät kohti uusia prosessivaihtoehtoja päästöjen vähentämiseksi. Työssä tutkitaan raaka-ainepanosten vaikutusta täysin vetypohjaiseen suorapelkistys-valokaariuuniprosessiin, jota ei ole vielä toteutettu teollisessa mittakaavassa. Työn tarkoituksena on saada ymmärrystä raaka-ainepanoksista ja reunaehdoista sopivan panoksen valitsemiseksi sekä mallinnuksen avulla tutkia eri panosten vaikutusta prosessiin sekä sen lopputuotteeseen.

Työn kirjallisuusosiossa esitellään teräksen nykyiset tuotantoprosessit sekä tutkittavan prosessikonseptin raaka-aineet sekä suorapelkistyksen kemiallinen perusta ja toteutusmahdollisuudet. Myös mahdollisia teknisiä haasteita esitellään työn kirjallisuusosiossa. Työn kokeellisessa osuudessa mallinnetaan prosessi HSC-simulointiohjelmistolla sekä esitellään mallin tuottamat tärkeimmät tulokset ja verrataan niitä nykyisiin prosesseihin. Mallilla simuloitiin eri skenaarioita, joissa muutettiin rautaoksidipellettien laatua sekä panostetun romun suhdetta panostettuun rautasieneen. Työssä tarkastellaan raaka-ainepanosten vaikutusta muun muassa syntyvän kuonan määrään, energiankulutukseen, hiilidioksidipäästöihin ja tuotteen puhtauteen. Saadut tulokset osoittavat, että prosessille on hyödyllistä käyttää hyvälaatuisia pellettejä sekä rautaromua siinä määrin kuin sitä on saatavilla ja kun tuotteen vaatimukset sen sallivat. HSC-ohjelmisto soveltuu prosessin yksinkertaiseen massa- ja energiatase pohjaiseen mallinnukseen, mutta prosessin tarkempi mallinnus vaatisi enemmän teollisen mittakaavan tietoja prosessista sekä mahdollisesti kehittyneemmän simulointiohjelmiston.

Avainsanat Teräs, Vetypelkistetty teräs, Valokaariuuni, Kuilu-uuni, Mallinnus, Simulointi, HSC

Table of contents

Symbols and abbreviations

Symbols

%	Percent
H	Enthalpy [J/mol]
Nm^3	Nominal cubic metre
Vol.%	Volume percentage
Wt.%	Weight percentage

Abbreviations

AEL	Alkaline water electrolysis
BF-BOF	Blast furnace – Basic oxygen furnace
CDRI	Cold direct reduced iron
DRI	Direct reduced iron
EAF	Electric arc furnace
GHG	Greenhouse gas
GOD	Gas oxidation degree
H_2-DRI-EAF	Hydrogen based direct reduction - electric arc furnace
HBI	Hot briquetted iron
HDRI	Hot direct reduced iron
HMS1	Heavy melting steel 1
IEA	International Energy Agency
IIMA	International Iron Metallics Association
IO	Iron ore
NG	Natural gas
OPEX	Operating expense
PEM	Proton exchange membrane electrolysis
RES	Renewable energy sources
RHF	Rotary Hearth Furnace
SEC	Specific energy consumption
SMR	Steam methane reforming
SOEC	Solid oxide electrolysis
TLS	Ton of liquid steel
TRL	Technology readiness level

1 Introduction

Steel is one of the cornerstones of the modern economies and present in our daily lives for example in vehicles, infrastructure, machinery and electronics. However, currently the steel production is accountable for 7-9% of the global carbon dioxide emissions [1]. Thus, as the global attention shifts towards more sustainable practices, the steel industry faces a significant challenge and transformation as they strive to make their steelmaking operations more sustainable. In addition, legislative pressure such as the Paris agreement in Europe with the goal of reducing greenhouse gas emission by 80-95% until 2050 acts as a major driver for the steel industry's green transition [2].

Currently, carbon intensive blast furnace-basic oxygen furnace process is the most common process for the production of steel from iron ores. Steelmakers across the globe has thus had a strong effort in investigating ways of producing steel in a more sustainable method. Given that the blast furnace process is operated close to its thermodynamic limits, novel production methods have been researched in order to find possibilities to reduce the CO_2 emissions [3]. One exceptionally interesting process which has led to multiple projects by steel companies is the hydrogen direct reduction process that is paired with an electric arc furnace (H_2-DRI-EAF process). It is based on an existing natural gas direct reduction process with the exception that the natural gas is completely or mostly replaced by hydrogen gas. By doing so, the reduction process can be carried out in a manner that only emits water vapour instead of carbon dioxide. However, the hydrogen direct reduction process has not been demonstrated on an industrial scale, and its technological development is still in progress, with widespread adoption still years away.

The aim of this thesis is to study the effects of raw materials in the H_2-DRI-EAF process and the liquid steel that is the product exiting the system boundary. As of now, very scarce amount of research has been published on the simulation and modelling of the completely hydrogen-based process. Thus, a simulation flowsheet was built using the Metso's (former Metso-Outotec) HSC-simulation software [4]. The built simulation model was used to study the effects of different raw material charges on the process conditions and the end product. Table 1 shows the research objectives, questions and methods of this thesis.

Table 1. The research objectives and questions addressed in this Master's Thesis

Research Objectives	Research Questions	Research methods
To understand and assess the H_2-DRI-EAF process and its raw materials.	What is H_2-DRI-EAF process and what raw materials are used?	Descriptive
Find possible challenges in the widespread implementation of the process.	Which factors impose challenges for the implementation? What issues are posed by the raw materials?	Descriptive
To design and build a simulation flowsheet utilizing HSC software.	Can you simulate the H_2-DRI-EAF process accurately using HSC Sim?	Quantitative
Study the effects of raw materials by means of simulation.	What is the optimum raw material and what are the boundary conditions for the selection?	Quantitative

The thesis scope is narrowed to examine the effects of iron ore pellet quality and the charged amount of steel scrap on the production process. With the finding of the literature review being used in the experimental part as different kind of modelling values and assumptions. The aim is to gain understanding on how different raw materials affect the process and to be able to discuss some of the criteria that raw materials should be considered for the process. Matters like the energy consumption, produced slag volume and emissions are used when quantifying the feasibility of the charge.

LITERATURE REVIEW

2 Overview on steel

This chapter begins by introducing the steel material and its increased global production capacity. This is followed by a brief preview on the current industrial production processes which acts as a benchmark for the new technologies. Some of the issues related to the state of art processes are discussed in order to better understand the drivers for a change in the ironmaking and steelmaking industry. The chapter ends by discussing some of the relevant projects related to hydrogen-based steelmaking.

2.1 Steel in modern economy

Steel is the most important engineering and construction material in the world due to its high tensile strength and relatively low cost. Steel is an alloy of iron and carbon that contains less than 2% carbon and 1% manganese and other trace elements such as silicon, phosphorus, sulfur and oxygen. [5]. The various applications of steel results in the need of producing different types of steels and thus various grading systems are implemented to distinguish between them. World Steel Association [5] states there are over 3 500 different grades of steel with varying chemical compositions resulting in different material properties.

World's population has grown over the past decades along with the overall economic growth resulting in the increase in demand and thus production of steel globally. Most of the steel produced is consumed by construction and transportation sector so it is reasonable to state that the demand of steel greatly depends on the world's gross domestic product (GDP). The International Energy Agency (IEA) [6] forecasts that the continuing economic growth especially in regions such as India, ASEAN countries and Africa would result in continued growth in steel demand even when the demand in Chinese markers gradually declines. The increase in the global crude steel production as well as the increase in world's population is shown on the Figure 1. The production of steel has more than doubled from 2000 to 2022 with compound annual growth rate of 3.7% in the specified timeframe.

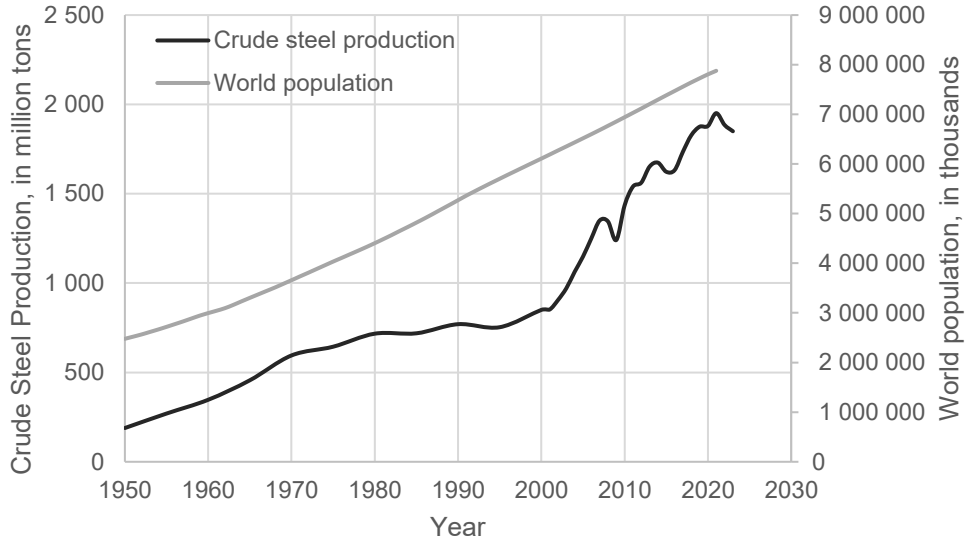

Figure 1. The development of crude steel production and the world's population from 1950 [7], [8].

According to the World Steel Association, in 2023 China produced 55% of the crude steel produced in the world [8]. China is the largest producer of steel with the majority of the steel used to meet domestic demand and to allow for modernisation of its construction, infrastructure and industrial sector [9]. Thus, it is clear how China's transition towards cleaner steelmaking practises will have a vast impact on global emissions. As illustrated in Figure 2, excluding Asia and Oceania the rest of the world only produces roughly one quarter of the steel.

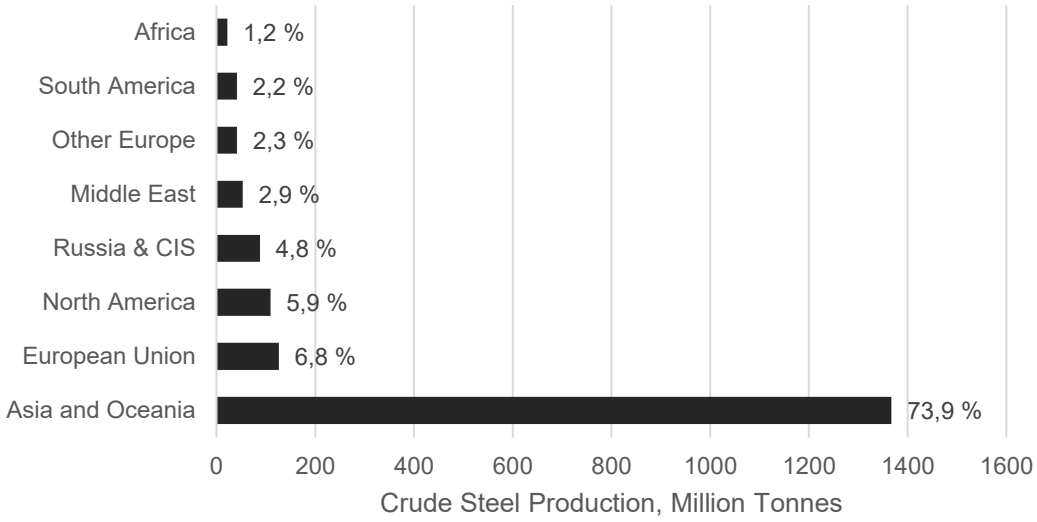

Figure 2. Global steel production geographically in 2023 [8].

2.2 Currently used production processes

Steelmaking is often divided into two categories based on their raw material: primary route and secondary route. Blast furnace-basic oxygen furnace (BF-BOF) is considered a primary route of steelmaking as it uses iron ore as raw material. While as electric arc furnace (EAF) is referred to as a secondary route of steelmaking as it uses mainly recycled scrap as raw material but also sponge iron or pig iron can be used as a charged material [10]. Currently 70% of the steel produced globally is produced by the BF-BOF process route. It is regarded as a highly optimized process that is operated close to its thermodynamic limits with technological advancements driven by ecological and economic factors implemented throughout its lifetime. The remainder (roughly 30%) of the produced steel is mainly obtained from the Electric Arc Furnace process [11].

Blast furnace is a continuously operating tall vertical shaft furnace in which iron oxide (IO) containing material is reduced to metallic iron by using coke as a main reducing agent. It is a counter current process where the IO material descends, and carbon monoxide rich reaction gas formed according to Equation (1) rises up in the furnace. As the burden descents in the furnace, it undergoes through various chemical reactions in the upper, middle and lower part of the furnace and the temperature rises when moving downwards in the blast furnace. The reactions of iron oxides that takes place in stages (hematite → magnetite → wüstite → metallic) in a blast furnace is shown on Table 2 and the net reduction reaction in Equation (6). Stoichiometrically, the production of 1 ton of iron requires 0.8 tons of CO and 1.4 tons of Fe_2O_3. In this process, 1.2 tons or 635 Nm^3 of CO_2 is produced as a byproduct. Finally, at the bottom of the furnace denser hot metal phase and less dense slag phase can be tapped out [11].

$$2C(s) + O_2(g) \rightarrow 2CO(g) \quad (1)$$

Table 2. The reduction reactions that occur in a blast furnace, enthalpies from HSC Rea-module. [4], [11]

Reaction equation	Enthalpy [kJ] 298K	Enthalpy [kJ] 843K	Eq. No.
$3Fe_2O_3 + CO(g) \rightarrow 2Fe_3O_4 + CO_2(g)$	-39.6	-24.8	(2)
$Fe_3O_4 + CO(g) \rightarrow 3FeO + CO_2(g)$	37.4[1]	20.5[1]	(3)
$FeO + CO(g) \rightarrow Fe + CO_2(g)$	-17.9[1]	-21.7[1]	(4)
$Fe_3O_4 + 4CO(g) \rightarrow 3Fe + 4CO_2(g)$	-16.3[2]	-44.6[2]	(5)
$Fe_2O_3 + 3CO(g) \rightarrow 2Fe + 3CO_2(g)$	-24.1	-40.0	(6)

[1] Occurs at temperatures T>570°C

[2] Occurs instead of reactions given in Equation (3) and (4) at T<570°C

The carbon saturated hot metal also referred to as pig iron contains typically around 4.5 wt.% carbon and significant amount other impurities such as silicon which deteriorates the properties of the material [12]. The content of carbon is significantly reduced, and various impurities are controlled to a desired level in a downstream converter process. Typical converter process is the basic oxygen furnace (BOF) process. The batch process conducted in a barrel shaped, refractory lined vessel, begins with charging the hot metal, slag formers and scrap metal into the furnace. This is followed by (supersonic) oxygen blowing that oxidises the impurity metals from the hot metal phase to the liquid slag phase. Finally, the produced steel and slag can be tapped out of the furnace [11].

The remainder, roughly 30%, of the steel produced globally is mainly produced via Electric arc furnace route. The EAF is a batch process that melts and refines the charged ferrous scrap material. It is conducted in a refractory lined vessel and the process begins with the charging of the raw materials and the slag formers. Usually, steel scrap is used but also DRI or hot metal can be used as an iron bearing material. The charge material is heated by using electric power and by lowering the graphite electrodes into the furnace. The heating is often assisted by introducing chemical energy by injecting oxygen, carbon containing material and using natural gas burners. The melting is followed by the refining stage where the composition of the heat is adjusted, and the impurities move to the slag phase. Finally, the steel and slag phase can be tapped out separately of the furnace [11], [10].

However, the introduced BOF and EAF requires some additional refining steps referred to as secondary metallurgy to meet the requirements of high-quality steel grades. Thus, various process steps between the primary processes and casting are required in order to refine the steel to its final composition. Most common refining processes include deoxidation, desulphurization and degassing that are conducted based on the requirements set for the produced steel grade. These process steps are usually carried out in ladles by using inert gasses, deoxidating and desulfurizing elements and with the help of vacuum treatment. [11]

2.3 Issues related to current steelmaking practises

Steel production is a major source of global greenhouse gas (GHG) emissions due to the CO_2 produced in the reduction process of iron ore material when coke or other carbon containing substances are used as a reductant. Global steel production is responsible for 7-9% of global CO_2 emissions which is the highest share among heavy industries. Nowadays, the steel and iron sector's annual carbon dioxide emissions are 2.6 Gt [1]. For reference The International Energy Agency reported that in 2022 the carbon dioxide emissions caused by chemicals industry, passenger cars and aviation were 1.3 Gt, 3.0 Gt and 0.8 Gt respectively [13].

The Institute for Energy Economic and Financial Analysis [14] states that the BF-BOF process releases the greatest amount of carbon dioxide emissions per produced ton of steel. As it currently is the most common way of producing crude steel, we can clearly see the urgency of shifting away from that technology into processes that are not so carbon intensive. The natural gas-based direct reduction production route seems to emit roughly half the amount of CO_2 when compared to BF-BOF. However, benchmarking the DRI-EAF process with Scrap-based EAF, we observe that currently the scrap-based steelmaking route has the lowest CO_2 intensity. Table 3 compares the CO_2 emissions released by using different production processes. The indirect emissions refer to the GHG emissions caused by the generation of the consumed electricity. Thus, the development of the steel industry is strongly linked to the supply and availability of renewable energy.

Table 3. Steel production carbon dioxide emissions with different process routes [14].

Process	Direct and Indirect CO_2 (t)/Crude steel (t)	Share of global steel production
BF-BOF	2.2	73.2%
DRI-EAF	1.4	4.8%
Scrap-EAF	0.3	21.5%

Table 3 indicates that currently the scrap-EAF process route is the most sustainable which has been a substantial driver in the European steel industry's transition from the BF-BOF process to EAF based steelmaking. However, the EAF process using solely scrap material cannot meet the markets demand for steel. As visualised in Figure 3, IEA [1] states that currently iron ore is the source for approximately 70% of the metallic raw material globally with the rest being steel scrap. In the future, recycling is not enough, and iron ore is still needed to produce enough steel. SSAB [15] estimates that in 2050 50% of the metallic raw material will be iron ore with the rest being steel scrap.

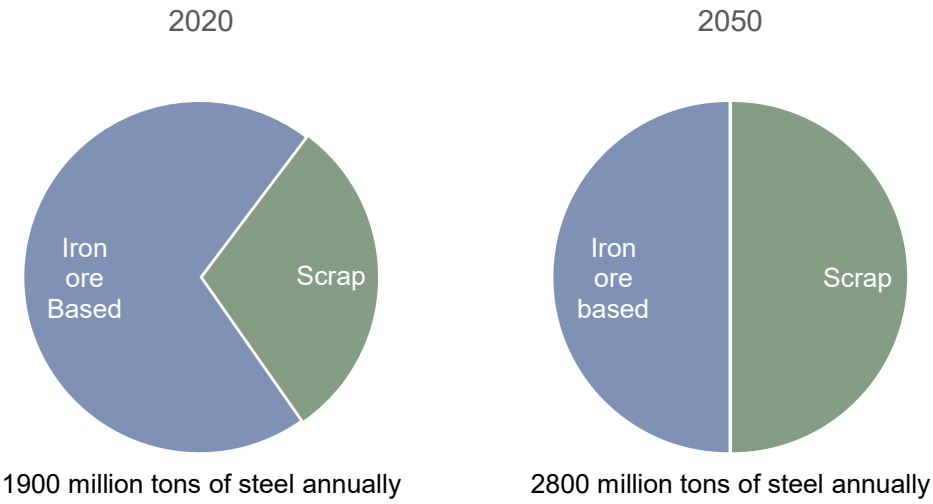

Figure 3. Estimation highlighting the need of iron ore-based steelmaking in the future [1], [15].

Another issue with using scrap material is the cumulative enrichment of impurities that cannot be removed from the steel in a feasible manner. These are referred as “tramp elements” which of copper and tin are the most important that origins from for example electronics. Even small amount of these impurities weakens the material properties of steel. Copper in steel causes hot shortness that leads to surface cracking when over 0.1 wt.% Cu is present. Tin aggravates these phenomena even at concentrations as low as 0.04 wt.% [16].

In addition to carbon dioxide emissions, the economic aspect may drive the steel production towards new emerging technologies such as the H_2-DRI-EAF process. For example, the EU emissions trading system results in a price for carbon dioxide emissions with the aim of creating an incentive for the industries to reduce their emissions. The average price of carbon dioxide in European Union was 14.6 €/tonCO_2 in 2010 and it increased drastically to 85.2 €/tonCO_2 in 2022 [17]. The increase in the price of CO_2 emissions and on the other hand, the decrease in the price of H_2 due to technological advancements leads to new sustainable steel producing processes to be more cash cost optimal than the conventional BF-BOF process. However, it must be noted that when utilizing solely hydrogen produced electrolytically the cost of the final steel product greatly depends on the current price of electricity.

Although, the act of producing steel in a more environmentally manner is a large global trend that has gained popularity also in the press, it is important to pay attention to the terminology used. The term ‘Green Steel’ does not have a universal definition, so each party may have their own definition of the

term. This can lead to misunderstandings and even 'greenwashing' as steel producers are under pressure to make their operations more sustainable. Also, as for example Muslemani et al. [18] highlighted, it is important to distinguish between steel products that have low greenhouse gas emissions and "low-carbon steel" which refers to existing type of products with minimal carbon content (0.04-0.40 wt.%).

2.4 Ongoing projects in hydrogen-based steelmaking

Currently the hydrogen-based reduction of iron ores is still in its infancy on an industrial scale. In 2020 IEA rated the direct reduction of iron oxides using solely H_2 as Technology readiness level 5 (Large prototype, Components proven in conditions to be deployed) [9]. Thus, steelmakers are launching major projects to develop hydrogen-based steel production processes to leverage hydrogen economy. The currently released projects are typically designed to have a capacity of around 2.5 million tons of liquid steel per year [19]. The following paragraphs discuss the ongoing projects in Europe regarding shaft furnace hydrogen based DRI production and their current outlook.

HYBRIT (Hydrogen breakthrough ironmaking Technology) is a strategic alliance formed in 2016 by three large Swedish companies: SSAB, LKAB and Vattenfall. The Alliance's mission is to pursue the transition towards fossil-free steel value chain by utilizing green electricity and hydrogen in their processes. In 2018 a pre-feasibility study of the chosen shaft furnace process was completed, and the main results were that HYBRIT faced no serious technical barriers and that the cost of HYBRIT steel is estimated to be 20-30% higher than steel produced with traditional practices and strongly dependent on prices of metallurgical coal, electricity and CO_2 emission rights. Hydrogen is used in a shaft furnace process as a reducing gas and Tenova HYL was chosen to supply its DRI technology. Currently, the shaft furnace process is paired with downstream EAF process. The DR process was demonstrated in June 2021 in Luleå, Sweden and the aim is to begin fossil-free commercial deliveries in 2026. [20], [21], [22]

A Swedish company H2 Green Steel was established in 2020 with the mission of rapid and remarkable reduction of carbon emissions in the steel production. The company's process concept is based on water electrolysis and hydrogen direct reduction followed by downstream EAF process. Midrex was chosen as the DR technology supplier and SMS Group as a supplier for both EAF and the downstream hot rolling and finishing processes. The company is building a large-scale green steel plant with the aim of beginning production in 2025 in Boden, Sweden. [19], [21]

German SALCOS (Salzgitter Low CO_2 Steelmaking) project was formed in 2019 by Salzgitter and Tenova with the mission of near CO_2-free steel production. The low emission concept is also based on water electrolysis, hydrogen direct reduction and EAF process. Energiron ZR developed by Tenova and Danieli was chosen as a technology for the DR process. The project has a goal of full conversion to hydrogen-based steelmaking that allows the reduction of CO_2 up to 95% by end of 2033. [23], [24]

The tkH2steel project was launched in 2020 by a German Thyssenkrupp Steel company with the aim of producing more sustainable steel. The project is also based on the hydrogen direct reduction process scheme which is followed by a melting step. The project aims on starting up its first direct reduction plant followed by two melting units in 2026 with the annual capacity of 2.5 million tons of sponge iron. The project's plan is to first operate with natural gas, implement a combination process in 2028 and ramp-up with 100% hydrogen in 2029. Thyssenkrupp steel has a goal that their transformation to carbon-neutral steel will be completed by 2045 at the latest. [25], [26]

ULCOS (Ultra Low CO_2 Steelmaking) is a consortium of more than 40 European companies and organizations that investigates the technologies that would allow a drastic reduction in CO_2 emissions. Under the project technologies such as blast furnace with top gas recycling, electrolysis of iron ore and new smelting processes has been investigated. The hydrogen-based route investigated by ULCOS also utilizes electrolysis of water, DRI production in a shaft furnace and downstream EAF processing. In 2020 Patisson and Mirgaux [27] published an article under ULCOS project stating that a first version of a mathematical model named REDUCTOR was established in order to study the hydrogen reduction reactions in a shaft furnace setting. [28]

3 Direct reduced iron production in a shaft furnace

This chapter first reviews the raw materials that are used in the production of DRI in a shaft furnace: iron oxide pellets and hydrogen. This is followed by discussion on the direct reduction process and its current state in the industry. Thermodynamics and kinetics of the occurring reactions are discussed. Finally, commercial technologies for the direct reduction are introduced.

3.1 Iron Oxide pellets

The iron oxide (IO) material is introduced into the direct reduction shaft furnace process typically in the form of mechanically durable pellets rather than for example in a lump ore form. In the DR processes no melting or refining takes place, so all of the impurities in the feed material get concentrated in the final sponge iron product. To produce a purer iron oxide feed material, a more rigorous beneficiation process is required which generates fine IO material that in turn requires proper pelletizing (agglomeration and induration) before it can be used as a feedstock for the shaft furnace process. Currently, pelletizing is the only viable method of agglomeration, and the produced pellets can be divided into three categories: BF-grade pellets, DR-grade pellets and RHF-grade (Rotary Hearth Furnace) pellets based on chemical, metallurgical and physical properties [11], [10].

The main feedstock of a pelletizing process is iron concentrate that initially contains a large amount of residual moisture from the iron ore beneficiation process. First, the water is filtered from the concentrate and then additives like carbon, limestone/dolomite, and binders such as bentonite are mixed into the material. This is followed by the balling process where the pellet shape is formed. Balling process is typically done in a rotary drum or a rotary disc with the aimed pellet diameter of 8-13 mm. The product of the pelletizing drum is referred as green pellets as they still contain moisture and does not satisfy the strength requirements for a pellet to be fed into for example to a blast furnace or a shaft furnace. Thus, an induration process is required in which the pellets are hardened/indurated using elevated temperatures to achieve the required properties for charging and for storing [29], [30]. Some of the most important physical and metallurgical properties of IO pellet feed suitable for DRI production and their rationale are presented in Table 4.

Table 4. Desired physical and metallurgical properties of iron oxide pellets for direct reduction [29], [30], [31].

Property	Rationale
Diameter of 6 – 16 mm	Roughly the optimal size range that can provide consistent product quality with high metallization.
Minimum number of fines	Prevention by screening as fines cause high pressure-drop and move downwards towards the discharge of the shaft furnace promoting inconsistent product quality.
High strength	Pellet strength minimizes the fines generation. The strength of the pellet decreases notably when the diameter increases more than 12.5 mm.
High reducibility	Depends on porosity, particle size and chemical composition of the phases present. A low reducibility results in low metallization of the product.
Low degradation due heat	Degradation causes fines to move downwards to the discharge part of the shaft furnace.
Minimum amount of swelling	Mainly a concern when using carbon-based reductants. When swelling exceeds 20 vol.% it can cause issues to production and product quality.
Little tendency for sticking	Sticking can form clusters in the shaft furnace and compromise smooth DRI discharge and reducing gas flow.

The sticking of iron oxide pellets, also shown on Table 4, is a specific issue for direct reduction processes as the pellets do not melt in the reactor like in a blast furnace. Ling-Yun et al. [32] argues that the sticking among IO pellets is one of the most serious problems associated with gaseous shaft furnace process. As the sticking imposes a risk for a continuous operation in the shaft furnace, research efforts have been devoted to finding parameters that affect the sticking phenomena and on the other hand methods of prevention. According to [32], [31] and [33] the sticking of pellets is found to be strongly linked with the H_2 amount in the reducing gas atmosphere and the reduction temperature. Sticking decreases with addition of H_2 in the reducing gas and it can be quantified by using a sticking index. In 950°C the sticking index for volumetric fractions of H_2 in a H_2-CO mixture at 0, 0.44 and 1 were measured at 17.2%, 12.3% and 7.0%, respectively. The sticking tendency was found to increase as the reduction temperature increases. The agglomeration of pellets is not observed at temperatures below 600°C but the sticking phenomena increases clearly with temperatures of 950°C and reaches maximum at 1000°C. So, the sticking phenomena must be considered in typical shaft furnace process temperature which greatly exceeds the 600°C.

To combat the issue of IO pellet agglomeration a few methods have been found to be effective: higher basicity and gangue content in the pellet can reduce the sticking tendency. However, increasing the gangue content in the pellets leads to less iron production and unfavourable conditions in the up-stream EAF process. The prevention of the agglomeration phenomena can be done by coating the IO pellets by suitable coating compounds. Coating the pellets by SiO_2 (silica) or CaO (lime) was shown to decrease the sticking and the latter of which was proven to be more effective coating material. The amount of coating required is in the range of 5 kg per ton of feed material. It is still noteworthy that the coating of the pellets by these substances has an effect on the reduction process that must be considered [32].

Degree of metallization or metallization-% is an important parameter that is a quantitative measure of the amount of oxygen removed from the iron oxide material in the shaft furnace. It is defined as the ratio between metallic iron present and total iron present in the DRI as shown on Equation (7) and it affects the downstream EAF process such as its energy consumption and the slag volume that is formed. It is impacted by the reducing gas quantity and quality but also the gangue material in the iron oxide pellets. Fluidized bed-based hydrogen reduction process achieved metallization of 95% and HYL reference pilot plant utilizing 90% hydrogen gas as reducing agent achieved the metallization of 94-96%. The rest of the total iron being in the form of FeO [34].

$$Metallization - \% = \frac{wt - \%\ of\ metallic\ iron}{wt - \%\ of\ total\ iron} \tag{7}$$

The term 'DR-grade pellet' is not standardized but rather a trade term used in the industry. Currently the optimum composition of a pellet depends on specific plant conditions as for example the composition of the reducing atmosphere and the steel grades that are being produced. However, there are chemical properties that are specifically desired for the DR-grade IO pellets that are mostly dictated by the downstream EAF process. Total iron content of the IO pellet should be as high as possible as higher iron content means lower gangue content that has to be treated in the downstream processing. Typically, the iron content desired should exceed 67 wt.%. Also, generally the total amount of gangue should be less than 3-4% [35]. Typical chemical composition of the iron oxide pellet feed used in direct reduction and blast furnace processes are compared on Table 5.

Table 5. Chemical characteristics of typical iron oxide pellets used in direct reduction and blast furnace processes [11] [10].

Parameter (wt.%)	DR-Grade	BF-Grade	The DR-Grade pellet
Total Fe	65-69	63-65	Contains significantly more iron.
Total P	<0.03	<0.03	Equally low phosphorus content.
Total S	<0.01	<0.03	Equally low sulphur content.
SiO_2	0.9-1-0	2.5-5.3	Contains significantly less acidic gangue.
Al_2O_3	0.2-0.5	0.2-3.0	Contains significantly less acidic behaving gangue.
MgO	0.2-0.9	0.3-1.5	Contains less basic gangue.
CaO	1.1-1.2	0.6-3.6	Contains less basic gangue.
Reducibility index	92-95	91-97	Smaller range preferred.

In addition to the compounds listed in Table 5 research article by Ahmed et al. [36] listed some of the other impurities that were present in DR-grade IO pellets produced at LKAB's pilot induration furnace in Sweden. In the pellet, the total phosphorus content was 0.025 wt.% and the levels of K_2O, MnO, TiO_2, V_2O_5 and Na_2O were 0.03 wt.%, 0.07 wt.%, 0.18 wt.%, 0.20 wt.% and 0.03 wt.%, respectively. The pellet had an average diameter of 12.5 mm with total iron content of 67.8 wt.% and the basicity of 1.13 (B2) and 1.55 (B4). In a laboratory-scale experiment the hydrogen reduction yielded a metallisation of 90.4%.

The specific requirement on these basic components in the pellet is determined by the desired slag composition in the downstream EAF process. However, a meta study by Zakeri et al. [37] underlines the beneficial effect of CaO in the reduction rate and states that the effect of MgO can be beneficial or unfavourable depending on the phase that is formed during the reduction reaction. Thus, it is justified to use limestone for coating the pellets without compromising the reduction process. The basicity of a pellet or the slag formed in downstream processes is usually described by using two ratios: two component or four component ratios can be used according to Equations (8) and (9), respectively.

$$B2 = \frac{CaO}{SiO_2} \tag{8}$$

$$B4 = \frac{CaO + MgO}{SiO_2 + Al_2O_3} \tag{9}$$

Especially acidic gangue (SiO_2 and Al_2O_3) content in the IO pellets should be particularly low in order to ensure that the following EAF process is as efficient as possible. High content of acidic components leads to larger slag volume due to high fluxing need and lower metal yield as some of the iron is lost into the slag phase in the form of FeO [38]. From a reaction kinetic perspective, adding SiO_2 may lead to the formation of fayalite (Fe_2SiO_4) which lowers the rate of reduction. Despite being an amphoteric substance, alumina (Al_2O_3) exhibits acidic behaviour when interacting with basic slag. The effect of alumina depends on the amount present in the material. At alumina contents less than 1 wt.%, it was observed that the reduction rate decreased as the alumina content increased from 0.5 wt.% to 1 wt.% [37].

So, as discussed above, the successful direct reduction process is highly sensitive to the purity of the feed iron oxide material. International Iron Metallics Association (IIMA) [39] highlights the overall trend of declining iron ore quality in the last 20 years. The average iron content in the sinter feed has decreased from the 63.9 wt.% in the 1998 to the value of 61.9 wt.% that was reported in 2018. This in turn, means that the overall amount of gangue material has increased. In the same time period, the average SiO_2 concentration has increased from 4.11 wt.% to 5.16 wt.% and the Al_2O_3 amount has increased from 1.7 wt.% to 1.87 wt.%. Also, the phosphorus which is challenging to treat has been increasing from 0.048 wt.% to 0.067 wt.%. On the other hand, the iron ore pellet feed quality has remained rather the same, so this implies the increased focus for resource-intensive and costly beneficiation and ore concentration. So, it is important to consider the whole value chain of steel production when assessing its sustainability.

However, currently the focus seems to remain on using DR-grade pellets for the reasons provided earlier. In addition, the usage of BF-grade iron ore pellets has disadvantages such as lower liquid steel yield in the EAF, and increased fines generation which negatively impacts the process. These factors act as financial challenge on utilizing lower grade ores in the gas direct reduction processes. The comprehension of the influence of lower-grade iron ore pellets on the entire hydrogen-based process will further develop as industry participants conduct various pilot trials in the upcoming years. [40]

To allow the transition in the steel industry, the increasing demand in DRI produced steel must be matched by the sufficient supply of DR-grade iron oxide pellets. The scarcity of DR-grade pellets might pose a challenge for the decarbonization pathway for the steel industry, especially for the EAF process route. According to the international iron and metallics association (IIMA) the supply of merchant DR-grade iron oxide pellets is expected to increase from 38Mt in 2020 to 81Mt by 2030 [41]. Currently, the four largest miners of iron ore are: BHP, Rio Tinto, Vale and FMG that are expected to be

major players in supplying the DR grade IO pellets, even though currently having a focus on pellets used in the blast furnace. Some DR projects such as the HYBRIT secures the supply of suitable iron ore by having their own iron ore resources (LKAB). It remains to be seen how the global capacity of DR-grade pellets will increase and what will be the pricing spread of the various pellets.

3.2 Hydrogen

The hydrogen that the process utilizes as a reducing agent can be produced by using various feedstocks, energy sources and technologies. Currently, roughly 75% of the global hydrogen is produced from natural gas by means of steam methane reforming (SMR). This is commonly referred as 'grey hydrogen' or when combined with carbon capture and utilization as 'blue hydrogen'. However, turning natural gas (NG) into hydrogen emits GHGs, so the recent emphasis has been on producing hydrogen via electrolysis and by utilizing water and renewable energy sources (RES) as a feedstock. From a sustainability perspective, the 'green hydrogen' is the most promising process route because it ensures minimal GHG emissions [42].

Water electrolysis is a method for producing hydrogen by 'splitting' water molecules into hydrogen gas and oxygen gas by using electricity as a feedstock in the electrolyser. The electrolysis processes are divided into three different groups: Alkaline water electrolysis (AEL), Proton exchange membrane electrolysis (PEM) and solid oxide electrolysis (SOEC). These technologies differ by the type of electrolyte used. AEL utilizes two electrodes that are immersed in liquid KOH or NaOH and that are separated by a diaphragm to prevent the mixing of product gasses. In the PEM technology, a solid polymer is used as an electrolyte that allows both the proton transfer and separates the system so that the product gasses do not mix [43]. Finally, the SOEC technology that is the most recent one conducted in high temperatures. The state-of-the art electrolyte used in SOEC is yttria-stabilized zirconia that performs well in typical operating temperatures [44]. Schmidt et al. [45] reported that even though currently the consensus is that AEL is the preferred technology, a shift towards PEM is expected in 2030 due to cost effectiveness. A table comparing these hydrogen production technologies as well as the currently dominant natural gas-based route is presented in Table 6.

Table 6. A comparison on common hydrogen production technologies [46], [47], [48], [49], [50]

Parameter	SMR	AEL	PEM	SOEC
Feedstock	Natural gas, water	Water, electricity	Water, electricity	Water, electricity
Temperature and pressure	800-1100°C 25-30 bar	70-95°C 1-30 bar	≈70°C 1-35 bar	650-850°C <30 bar
Efficiency	70-85%	62-82%	67-84%	75-90%
Average USD/kg of H_2	2.1 2.3 (CCS)[1]	3.6-23.3[2]	3.6-23.31[2]	In development
Average kg CO_2 eq.	12.0 3.7 (CCS)[1]	Near zero with RES[3]	Near zero with RES[3]	Near zero with RES[3]
Power consumption kWh/m^3 H_2	Not Applicable	3.8-8.2 Typical industrial: 4.5	4.4-7.1	3.7
Maturity	Mature technology with references	Mature technology with references	Emerging technology with limited references	Emerging technology, no industrial references

[1] By Steam Methane Reforming with Carbon Capture and Storage
[2] Depending on the used energy source.
[3] Renewable Energy Sources

For the metallurgical process of reducing iron oxides by hydrogen, the production method of the hydrogen itself is not relevant. But the source of hydrogen has a great effect on the sustainability and the economics of the process. However certain requirements are set for the hydrogen to be used. Boehm et al. [51] states that the hydrogen can be produced using variety of different technologies including SMR and different electrolysis technologies. Also, it was stated that the purity requirements are relatively moderate and so allow a more flexible process with unreacted hydrogen recycling back to the process. The purity of hydrogen produced with different electrolysis systems can range from 99.6 vol.% to 99.95 vol.% on dry basis without treatment. Special treatment can be used to reach a purity of 99.998 vol.% and upwards. Specifications for hydrogen presented in the study by Boehm et al are presented in Table 7.

Table 7. Indicative set of requirements for hydrogen in the direct reduction process. [51]

Specification	Amount
Hydrogen amount	650 Nm^3/t DRI 58 kg/t DRI
Hydrogen purity	99.8 vol.%
H_2 pressure at top	≥4.5 bar(g)

In an industrial setting the hydrogen could be produced on-site or sourced 'over-the-fence' and transported to the production site. Hydrogen can be transported by utilizing pipelines, terrestrial vehicles, or maritime transport [52]. Currently, in industry, roughly 85% of the produced hydrogen is utilized at its production sites, and thus pipelines are mainly utilized for these short distance transportation scenarios [39]. However, there are challenges in transporting hydrogen as the small hydrogen molecule can penetrate small cracks, increasing the possibility of leakage and explosion hazard. Also, hydrogen can penetrate into steel materials causing hydrogen embrittlement. Pressure in the pipelines can vary from few bars up to tens of bars. Thus, combining all the previous topics, the transportation of hydrogen requires additional consideration especially when steel production sites are used to transport other fuel gases that do not pose the same risks as hydrogen [46].

3.3 Direct reduction

In the context of iron and steelmaking, direct reduction process refers to the act of reducing iron oxide material to metallic iron in the solid state by utilizing a reducing gas or carbon-containing substance. The iron bearing material is introduced in forms of forms of lumps, pellets or fines. [53]. The DR process is often classified as gas-based or coal-based depending on the reducing agent used. It can be carried out in for example rotary kilns, shaft furnaces or fluidized bed reactors [11]. Table 8 introduces common DR technologies to highlight that there is a variety of technological options.

Table 8. Comparison of the main technologies of direct reduction of iron oxides [11], [53], [54].

Focus of this study

Reactor	Reducing agent	Iron ore	Current commercial processes
Rotary kiln	Char, coal	Pellets & Lumps	SL/RN, Krupp-CODIR
Rotary hearth	Coal	Pellets & Lumps	Fastmet®
Fluidized bed	Carbon monoxide	Fines	Finmet
	Coal	Fines	Finex, Circofer
	Hydrogen	Fines	Circored
Shaft furnace	Carbon monoxide & Hydrogen	Pellets & Lumps	Midrex, Hyl/Energiron
	Carbon monoxide	Pellets & Lumps	Midrex, Hyl/Energiron
	Hydrogen	Pellets & Lumps	Midrex, Hyl/Energiron

The product of direct reduction processes is referred as direct reduced iron (DRI) or sponge iron. The name sponge iron is due to the fact that as oxygen is removed from the material in solid state, porous voids filled with air are left in the iron bearing material thus the material gets a sponge-like appearance. DRI can be in three different forms based on the application that it is later used for: Cold DRI (CDRI), Hot DRI (HDRI) or Hot Briquetted Iron (HBI). CDRI can be stored in dry places and used later at nearby steel plants whereas, HDRI can be transported to nearby EAF to utilize the heat content in the material, lowering the electricity consumption in the furnace. HBI is DRI that has been briquetted into a denser form. [10], [54].

A commonly discussed challenge associated with different forms of DRI is the reoxidation phenomenon. The exothermic oxidation reactions occurs when the DRI (especially HDRI) is in contact with oxygen to form hematite or magnetite thus lowering the value of metallization-%. Recent studies [42], [55] on 0 wt.% C hydrogen reduced pellets show that the phenomenon is elevated at high temperatures but that the oxidation is moderately low when the temperature decreases (0.07 wt.% increase in two days at ambient temperature). This can cause challenges in the product handling and storing. However, briquetting the product into HBI is a commonly used method of prevention that also facilitates the efficient maritime transportation [56]. The HBI form also can act as a buffer in case that the downstream melting unit cannot receive HDRI.

In 2022, the global production of DRI was 127.4 Mt which amounted to 6,8% of the total steel produced that year. Roughly 70% of the DRI was produced through a natural gas-based route with Midrex shaft furnace being the most commonly utilized technology [57]. Even though currently representing a marginal production volume, the DR processes have gained more attention in the recent years. This is due to the possibility of reduction of greenhouse gases, the possibility to utilize fines and the desire to avoid using volatilely priced metallurgical coke. The growing trend is also clearly visible in the number of global DRI projects as illustrated in Figure 4. Recently, the role of hydrogen has been emphasised in the new projects: either as 100% hydrogen-based projects or gradual shift towards hydrogen usage in the future. More announcements are likely expected for the time horizon of 2031-2035.

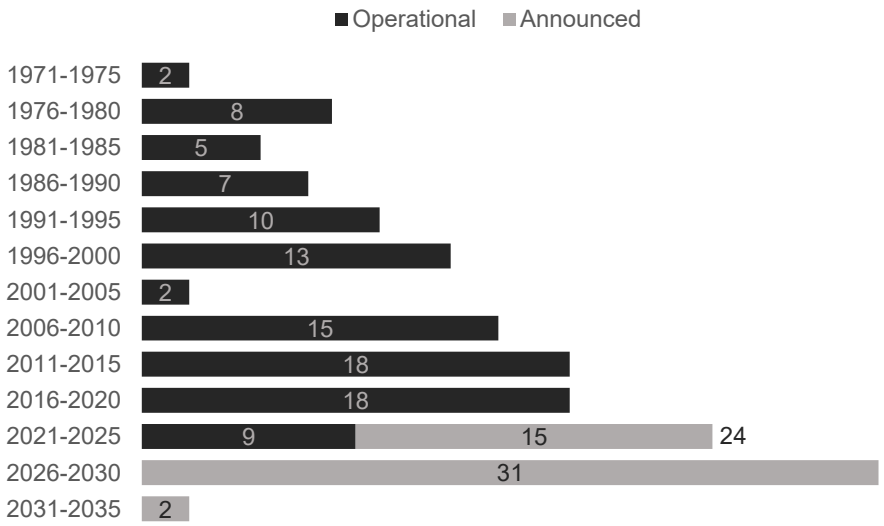

Figure 4. The number of operational and announced DRI projects according to beginning of production [58].

This study examines the direct reduction technology that utilizes only hydrogen as a reducing agent. This technology is perhaps the most interesting one as using hydrogen for iron oxide reduction emits no carbon dioxide. In addition, benchmarking the H_2-DRI-EAF process against the industry standard BF-BOF route, it offers a potential CO_2 reduction up to 95% when utilizing green hydrogen that is produced by using only renewable energy sources [59].

A vast majority of the produced DRI and HBI is used in EAF as is done in this study, but it can also be charged into BOF process for further refining [11]. In addition to that, Huitu et al. [60] conducted a techno-economical assessment on using DRI from the Midrex process as a partial substitute for IO pellets in a blast furnace. The results were promising as using DRI decreases the use of

coke in BF and thus decreasing the CO_2 emissions from the process. The feasibility of the process greatly depends on the NG price and the emissions allowance costs.

Furthermore, Gyllenram and Friesinger [61] argues that it would be especially efficient to use DRI in a blast furnace when lower grades of pellets are used. This is due to the fact that BF process has low iron yield losses to slag phase when in comparison with EAF. Friesinger, from Midrex, suggests that low grades of pellets should be fed into BF followed by BOF or alternatively to a special electrical smelter followed by BOF or EAF. The DR-grade pellets containing approximately 67 wt.% Fe would best be suitable for EAF operation. Therefore, it is not clear that the H_2-DRI-EAF process that is the selected technology of multiple projects as discussed in chapter 2.4 offers the best results when varying the oxide pellet quality.

3.4 Thermodynamics and kinetics

To understand the whole process behind hydrogen reduction and to be able to model and optimize it, it is important to study the thermodynamics and kinetics of the reaction itself. Baolin et al. [62] studied the reaction and reported that the reduction of Fe_2O_3 (hematite) happens through various steps depending on the temperature of the system. When the temperature is below 450°C the reaction happens stepwise from hematite to magnetite and finally to metallic iron according to reaction mechanism presented in Equation (10). When the temperature increases from 450°C, an intermediate compound called wüstite, Fe_xO becomes stable and must be also considered.

$$Fe_2O_3 \rightarrow Fe_3O_4 \rightarrow Fe \qquad \text{T<450°C} \qquad (10)$$

$$Fe_2O_3 \rightarrow Fe_3O_4 \rightarrow Fe_xO + Fe \rightarrow Fe \qquad \text{450°C <T<570°C} \qquad (11)$$

$$Fe_2O_3 \rightarrow Fe_3O_4 \rightarrow FeO \rightarrow Fe \qquad \text{T>570°C} \qquad (12)$$

Spreitzer and Schenk [63] concludes a few important remarks on the kinetics of hydrogen reduction system. First, hydrogen is a better reducing agent than carbon monoxide due to better kinetic behaviour in the system and as a smaller molecule it shows better diffusion behaviour through the iron oxide material. Secondly, an increase in the partial pressure of the reducing gas leads to a quicker reduction rate. Finally, as can be expected, the increasing the iron oxide particle size leads to lower reduction rates as the hydrogen gas has to travel longer distances by diffusion.

Figure 5 shows the Baur-Glässner diagram of a Fe-O-H_2 system created using FactSage 8.3 thermodynamic software [64]. It is a graphical representation

of the stability areas of different compounds depending on the system's temperature and gas oxidation degree (GOD). The 'GOD' that is presented in the x-axis of the figure is defined as a ratio between the molar fraction of water that is the oxidized gas component over the sum of molar fractions of hydrogen and water that are the oxidized and oxidizable gas components in the system as shown in Equation (13). The figure plotted by the FactSage programme corresponds with the results published by Spreitzer and Schenk [63] who studied the reduction of iron oxides and presented Baur-Glässner diagrams for both Fe-O-C and Fe-O-H systems that were investigated.

In Figure 5 the phases in the left of the figure, Fe and Fe(s2) refers to metallic iron in body-centered cubic (BCC) and face-centred cubic (FCC) crystallographic forms, respectively. The monoxide and spinel phases refer to the unreduced wüstite (FeO) and magnetite (Fe_3O_4) compounds, respectively. The ideal gas refers to the gas mixture present in the system that was calculated using the ideal gas assumption. Thus, we observe that when the GOD-ratio decreases, the reduction force in the gas system increases. From the figure we observe that in higher temperatures the stability area of metallic iron and wüstite increases, so according to thermodynamic principles the reaction should be carried out in highest possible temperature.

Also, from Figure 5 it can be seen that in typical shaft furnace temperature range of 850-950°C the GOD desired in the system would have to be less than 0.3 in order to make sure that iron is present at its metallic state in the final product. If we assume a binary mixture of hydrogen gas and water vapour, this implies that the mass percentage of water vapour should be less than 79.3 wt.%. So, from a thermodynamical perspective the reducing atmosphere can be quite flexible and contain considerable amount of water vapour and still thermodynamically favour the two metallic iron phases.

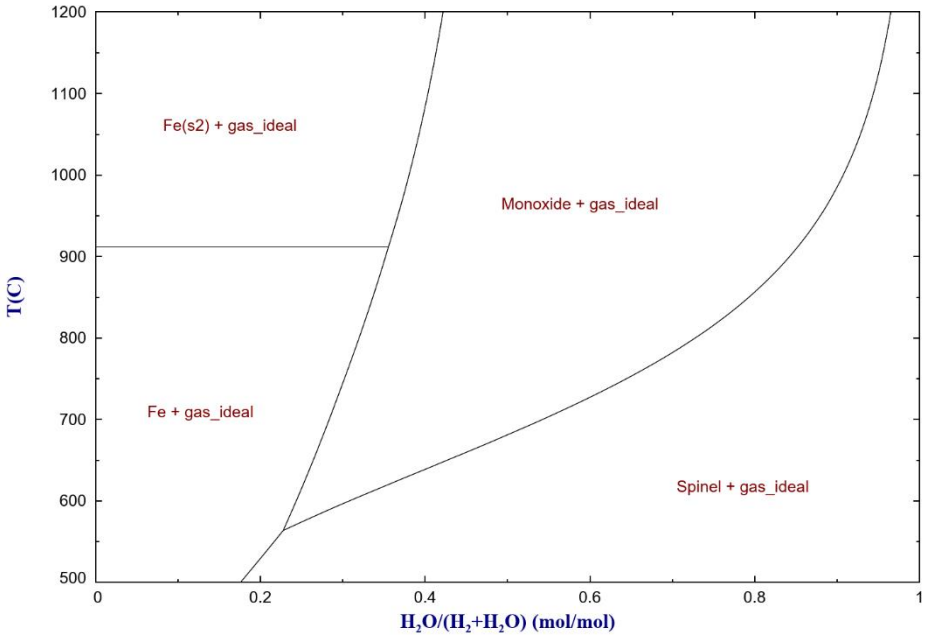

Figure 5. Baus-Glässner diagram for gas mixtures of H_2 and H_2O referred as 'GOD'-value presented in Equation (13). Plotted using Factsage 8.3.

$$GOD = \frac{X_{H_2O}}{X_{H_2O} + X_{H_2}} \tag{13}$$

As the industrial scale process happens on temperatures which far exceeds the thermodynamical limit of 570°C, the mechanism shown in equation (12) is the one of interest. However, it must be noted that temperatures exceeding 570°C improves the kinetics of the reaction but the temperature should not exceed the point where the pellets start to melt together. The reduction reactions are summarised in Table 9: the elementary reduction steps are shown in reaction Equations (14)–(16) and the overall reaction is presented in Equation (17). Jabbour and Nissrine [65] reports the importance of excessive amount of hydrogen gas in order to produce sponge iron. Otherwise, the reactions (14) and (15) become thermodynamically more favourable and only iron oxides Fe_3O_4 and FeO are being produced in the system. For complete reduction of iron oxide, a H_2:Fe ratio of 2 is reported in the study.

Table 9. The reduction reactions that occur in hydrogen reduction, enthalpies from HSC Rea-module [4], [65].

Reaction equation	**Enthalpy [kJ]**		**Eq. No.**
	298K	**1173K**	
$3Fe_2O_3 + H_2 \rightleftarrows 2Fe_3O_4 + H_2O(g)$	1.5	3.2	(14)
$Fe_3O_4 + H_2 \rightleftarrows 3FeO + H_2O(g)$	78.5	49.9	(15)
$FeO + H_2 \rightleftarrows Fe + H_2O(g)$	23.2	14.6	(16)
$Fe_2O_3 + 3H_2 \rightleftarrows 2Fe + 3H_2O(g)$	99.3	63.5	(17)

Thermodynamically the net reduction process using solely hydrogen is strongly endothermic, while as the net CO-reduction reaction that takes place in the upper part of the blast furnace process is exothermic. This poses technical challenges as due to the endothermic nature of the reaction it is necessary to provide external energy into the system. This can be done by heating hydrogen and IO material that are the reagents in the reaction to elevated temperatures. In a context of producing steel in a most environmentally friendly matter, the heating of these reagents would be done by using electrical heaters that are powered by renewable energy sources. Another approach is to use an inert gas like nitrogen to act as a heat carrier in the process [21], [66].

A parameter is needed in order to investigate the excess amount of hydrogen that must be supplied to the shaft furnace in order to compensate for the positive reaction enthalpy that is observed in the reactor. Lambda is defined as a ratio of hydrogen that is fed to the shaft furnace and the hydrogen that is consumed for the reduction of the iron ore. Lambda is shown on Equation (18). It is an important parameter on the heat and energy balance of the process, and it is set so that the shaft furnace produces product with desired properties such as metallization.

$$\lambda = \frac{H_2\ feed\ to\ shaft}{H_2\ required\ for\ compelete\ reduction\ of\ iron\ oxides}\ [\frac{mol}{mol}] \quad (18)$$

3.5 Current commercial technologies for H_2 DR shaft furnaces

As introduced in Table 8, there are two high technology readiness level (TRL) processes for shaft furnace direct reduction: Midrex and Energiron. Both technologies utilize natural gas steam reforming to generate reducing agent that is used to reduce IO pellets or lump iron ore. The reducing agent generated is syngas which consists of carbon monoxide and hydrogen in various ratios. Both processes work counter-currently, as the charge material is loaded from the top of the reactor shaft and descends by gravity. The syngas is fed from the middle of the shaft furnace and rises upwards through the IO material. The reduction itself happens in the upper part of the furnace in a series of reduction reaction steps. The DRI product is allowed to cool down in the lower part of the furnace and discharged from the bottom of the shaft furnace. The carburization of the DRI depends on the composition of the reduction gas atmosphere and can range between 0.5-4% [67].

The Midrex direct reduction ironmaking is a fairly matured technology which was developed by the Midland-Ross Co. The first commercial plant was launched in 1969 in Portland, Oregon with capacity of 300 000 t/a [68]. In 2023 [59] the company's offered three process concepts with varying reducing atmospheres: Midrex NG which uses solely natural gas, Midrex flex which utilizes both NG and H_2 and finally Midrex H_2 designed to utilize only hydrogen. The main components of the Midrex NG process, which is illustrated in Figure 6, are the shaft furnace, NG reformer and a cooling gas system. The reducing gas is produced in the reformer via a continuous nickel catalysed steam reforming with fed natural gas and CO_2 and H_2O recirculated from the top gas as reagents. Typically, the reducing gas exits the reformer at 850°C with controlled H_2/CO ratio of 1.5 to 1.8. The shaft furnace used typically has a diameter ranging between 4 to 7 meters. The reduction reactions occur in the upper section of the furnace at temperatures reaching 950°C, after which the burden descends into a transitional zone and finally into a cooling zone. In the cooling zone, the produced DRI is cooled with a flow of cooling gas. Ultimately, the product is CDRI produced which is cooled by DRI cooler, HDRI to be utilized immediately in upstream processes or the DRI can be briquetted into HBI.

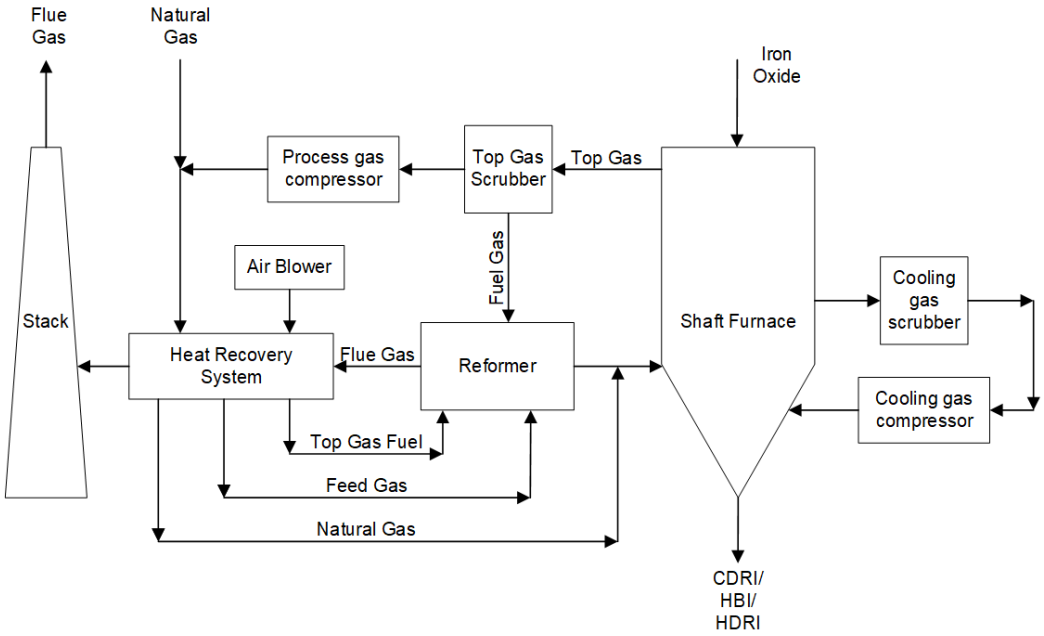

Figure 6. A simplified process flowsheet of the Midrex process, based on [69].

Hylsa steel company in Mexico (now owned by Tenova) developed HYL III shaft furnace process which was later rebranded as Energiron due to alliance formed by Tenova and Danieli. HYL III represents the third generation of the DRI process and was the first continuous process concept conducted in a shaft furnace. The first industrial plant utilizing the process was launched in

1980 in Monterrey, Mexico. The HYL III process is similar to the Midrex process with the main process components being a shaft furnace, a NG reformer and a cooling system. However, some of the key differences between the Midrex process and Hyl III process are: HYL utilizes a reducing gas richer in H_2 and the pressure in the shaft furnace is higher, up to 4-6 bar compared to 1.5 bar. Another generation of the process referred as HYL IV or HYL ZR ('Zero Reformer') is a newer process that does not require a separate gas reformer unit. In the HYL IV process both the reduction of iron ores and NG reforming occurs inside the reactor and the hot DRI serves as a catalyst for the reforming reaction [70]. A comparison of the current industrial shaft furnace processes running on a mixture of CO and H_2 is presented in Table 10.

Table 10. A comparison of the most commonly utilized shaft furnace direct reduction processes [70], [54], [59], [68]

Parameter	**Midrex**	**Energiron/HYL III**
Temperature (Reforming gas)	750-900°C	900-950°C
Pressure (Reforming gas)	1.5 bar	4-6 bar
Reforming	External reformer	External reformer/No external reformer with HYL ZR.
H_2:CO-ratio	1.5-1.8	3-5
Readiness for use of 100% H_2	With minor changes to existing process. Project ongoing with HYBRIT alliance.	With minor changes to the existing process. Project ongoing with H2 Green Steel and Salcos.
Discharge temperature (HDRI)	700°C	>600°C
DRI Metallization	93-94%	92-95%

When solely hydrogen is used in the direct reduction process, no natural gas reforming is required. Thus, the flowsheet of Midrex and HYL processes would simplify and become almost identical. However, both of these technology suppliers put emphasis on the flexibility for different reducing agents on the process. The flexibility in the process can be seen attractive as the availability of green hydrogen can be scarce depending on the geographical area. A more in-depth process description of H_2-DRI-EAF process that is simulated is discussed in chapter 6.1.

4 Electric Arc Furnace process utilizing DRI and scrap

This chapter first discusses the raw materials that are used in the electric arc furnace process that occurs after the shaft furnace. These raw materials are steel scrap, carbon containing materials and slag formers. Finally, the possible challenges when using carbon free DRI in the electric arc furnace are discussed.

4.1 Scrap used in EAF

In addition to iron oxide pellets, scrap is an essential iron bearing raw material in the H_2-DRI-EAF process concept. DRI and scrap can be charged with varying ratios to the Electric Arc Furnace process. When both DRI and scrap are used as a raw material several advantages can be leveraged compared to only charging the electric arc furnace with 100% DRI or 100% scrap. The tramp elements such as copper and tin present in the steel scrap can be diluted by the addition of DRI material to a tolerable level. This dilution makes it possible to utilize cheaper, lower grade and more available ferrous scrap to optimize the quality of the steel. [71]

The amount of scrap used in industrial DRI-EAF processes varies and according to Gyllenram et al. [72] three main trends in scrap use can be identified. Firstly, integrated DR-EAF process which uses mainly DRI as a charge material and only minor part of scrap for example just internal rejects in downstream processes are melted in EAF with the DRI. This approach has benefits such as predictable chemical composition of the produced steel and low tramp element content. However, solely charging DRI leads to increased power consumption, prolonged tap-to-tap times and larger slag volumes in the EAF which impacts the feasibility of such operation. Secondly, a more balanced charge of DRI and scrap can be utilized by for example charging one basket of scrap to every heat 'one-basket plant'. And finally, a scrap-based DRI-EAF plant that uses DRI only to dilute the amount of tramp elements present in the scrap.

Elkader et al. [73] studied the effects of different scrap and DRI ratios on an industrial EAF process with the capacity of 185 metric tonnes. Even though, the DRI had an average carbon content of 1.3 wt.%, the results can be considered as indicative for the hydrogen-based process. The process gas had 69 vol.% H_2, 18 vol.% CO, 5 vol.% CO_2, 5 vol.% CH_4 and 2.2 vol.% of N_2 [74]. The main results were that increasing the amount of DRI versus medium grade scrap, significantly decreased the content of sulphur and phosphorus as well as the total amount of tramp elements (Cr, Ni, Cu, Sn). Also, downsides in

increasing the amount of DRI charged to EAF were reported in the study. The consumption figures per ton of steel for lime, dolomite and carbon increased and the slag volume increased due to the higher gangue content in the sponge iron. In addition, the electric power consumption increased when the DRI in the charge mix increased. A power consumption of 384 and 500 kWh/t were reported when the amount of DRI varied from 0% to 80%, respectively. This is aligned with other studies, such as Kirschen et al. [75] reporting that the electrical energy demand increases close to linearly with the share of DRI in the charge mix greatly affecting the feasibility of operations. However, it must be noted that when only scrap is charged into the EAF, natural gas burners are utilized more. Also, the tap-to-tap time is shorter when scrap is utilized, typically ranging from 40-60 min compared to a case where mostly DRI is charged, typically ranging from 60-80 min [75].

There are over 3 500 different steel grades with varying chemical compositions thus resulting in a diverse portfolio of steel scrap available for the steelmaking processes. Also, the steel scrap is derived from various sources with different maturities so physical and chemical properties vary resulting in the fact that each piece of scrap is seldom like another. Therefore, it is essential to sort the scrap into different categories to make reusing the ferrous material easier. In the European Union, EFR has developed the "The EU-27 Steel Scrap Specification" framework in order to sort steel scrap into different grades. Regarding the chemical composition the framework has aimed analytical contents for the important tramp elements: copper and tin but also for alloying elements such as chromium, nickel and molybdenum [76]. However, it must be noted that unfortunately as of now there is not a global agreement on a classification system for ferrous scrap. Still, especially the producers of special grades steels often have their own sophisticated scrap sorting systems implemented in their production sites.

Broadly speaking, the scrap used into EAF processes is often divided into three categories based on their origin and purity: obsolete scrap, industrial scrap and internal scrap (in ascending order or purity). Obsolete scrap is ferrous material from consumer products such as old cars, appliances and machinery. Industrial scrap is generated during processing of steel strips or bars. And finally internal scrap is generated from the steel mill itself from for example quality rejections and tundish bottom. [11] Table 11 compares some of the physical and chemical properties of two commonly used ferrous scrap types: heavy melting steel 1 (HMS1) and shred steel scrap.

Table 11. HMS1 and shred comparison based on their chemical composition [11]

Parameter	HMS1	Shred	Comparison
Density, t/m^3	0.6	0.75	Shred has lower bulk density
Fe, wt.%	93.80 %	95.20 %	Shred has notably more total iron
Gangue, wt.%	2.34 %	1.97 %	HMS1 has more gangue
C, wt.%	0.22 %	0.60 %	Shred is notably more carburized
O, wt.%	1.48 %	0.40 %	HMS1 has notably more total oxygen
CaO+MgO, wt.%	1.04 %	0.63 %	HMS1 has more basic gangue
Al_2O_3+SiO_2, wt.%	1.30 %	1.34 %	Similar levels of acid gangue
P, wt.%	0.02 %	0.05 %	Similar levels of total phosphorus
S, wt.%	0.04 %	0.04 %	Similar levels of total sulphur
Mn, wt.%	0.66 %	0.43 %	HMS1 has more total manganese
Si, wt.%	0.16 %	0.30 %	Shred gas more total silicon
Cu, wt.%	0.16 %	0.25 %	Shred gas more total copper
Ni, wt.%	0.07 %	0.06 %	Similar levels of total nickel
Cr, wt.%	0.11 %	0.19 %	Shred gas more total chromium
Sn, wt.%	0.01 %	0.02 %	Similar levels of total tin
Mo, wt.%	0.03 %	0.01 %	Similar levels of total molybdenum

As can be seen from the Table 5 and Table 11, the chemical composition of scrap and DR-grade pellets differ from each other in a few ways. The scrap has a substantially higher total iron content than the iron pellets which is because the total oxygen content in the scrap is low. The overall impurity content in the scrap material is relatively low which in turn yields a lower slag volume in the downstream EAF. However, the scrap can have substantial amounts of tramp elements: copper and tin, the contents of which are detrimental for the steel quality and thus must be diluted. For example, Olatunde et al. [77] emphasises that when the copper content exceeds 0.22 wt.%, it notably weakens the mechanical properties such as tensile strength and hardness of construction steel. Currently, there are no commercial processes for the removal of copper and the energy consumption estimated for the process concepts are remarkable [78].

However, a major challenge with the use of scrap in industrial steelmaking operations is the availability and the price of the ferrous scrap of a suitable quality. Currently the largest consumers of scrap are EAF-based steel plants with the capacity in the range of 0.5-2.5 Mt per year and geographically the largest importers of ferrous scrap are Turkey, India and South Korea. On the other hand, the largest exporters of scrap are The European Union, USA and Japan. The availability of ferrous scrap is projected to increase globally so it is expected to be in a vital role in the decarbonization of the steel industry. Still, the increasing availability of scrap is not expected to match the increasing global steel production. [79]

4.2 Carbon containing material

In natural gas-based direct reduction processes the sponge iron contains significant amount of carbon that is referred as in-situ carbon in the downstream processes. Carbon content in DRI has a variable optimum; steel grade, production targets, and feedstock materials all play part in defining it in a case-by-case basis. However, the trend is to produce high-carbon DRI because of the additional chemical energy that it provides to the EAF [80]. On the contrary, the hydrogen reduced sponge iron does not contain any carbon and the charged scrap only contains little traces of carbon from contaminants such as paint and oil. Thus, carbon must be introduced to the process to carburize the steel and to create foaming slag in EAF to improve the energy efficiency of the process and to protect the furnace's refractory lining allowing for longer campaign life. In addition, the carbon in the furnace is used to reduce the FeO to metallic iron [81].

The current outlook is that there are multiple possible methods of introducing carbon into the H_2-DRI-EAF process. One approach is to use small amounts of natural gas in the shaft furnace in order to carburize the DRI to approximately a level of 0.8-1.2 wt.% C. This would imply that the reducing gas would have approximately 90 vol.% H_2 with the rest being carbon monoxide. But as this approach is not solely hydrogen based, but rather a modification of the existing gas-based DR process, it is excluded from the scope of the thesis. [80].

Another method is to feed the carbon into the EAF process. Carbon is introduced to the DRI by carburization phenomena, and in the context of hydrogen-direct reduction H-DR, two types of carbon can be identified: injected carbon and charge carbon. Solid carbon in the form of coal, petrol and coke are commonly used in the EAF. Carbon injection with oxygen to EAF is done via lances or injectors to generate CO bubbles that enable slag foaming, thus having a carbon with high reactivity ensures a good slag foaming practice. The minimum amount of carbon injected is 12-15 kg per ton of liquid steel. Charge carbon is added at the beginning of the heat and is charged in larger particles compared to injected carbon. When the aim is to carburize the melt, the charge carbon should have low enough reactivity, so the carbon is dissolved into the melt, rather than burned in the reactor. At the reaction temperature, the carbon is in form of iron cementite Fe_3C and graphitic carbon in various ratios depending on carburizing gas composition and temperature. [80], [81]

However, as the goal of the H_2-DRI-EAF process is to remarkably improve the sustainability of the whole process, it is important to substitute the fossil-based carbon materials in the EAF process. Thus, research efforts have been

devoted to finding alternative carbon sources for EAF steelmaking that are either renewable or recycled. Renewable biochar is converted from biomass via pyrolysis. Whereas using recycled materials is in line with the circular economy framework that utilizes the carbon present in recycled materials such as plastics and tires [81]. Table 12 is a summary of some of the possibilities and outlooks of alternative carbon sources in the EAF steelmaking.

Table 12. Current state of alternative carbon sources in EAF. [81], [82], [83]

Use	Carbon source	Current outlook
Injection carbon	Biomass based (untreated/biochar)	Further research needed on the effects of alternative carbon sources on the slag foaming practise. Challenges encountered in the use of 100% biochar, seems viable when mixed with coke. Blend of polymer and tyres with coke have been used in industrial trials at OneSteel successfully.
	Blend of rubber tire and fossil coke	
	Blend of polymer and fossil coke	
Charge carbon	Biomass based (untreated/biochar)	Promising results from industrial trials. The usage of biomass is technologically possible to implement. Rubber tires have been implemented on EAF steelmaking. Additional research needed for the complex stream of plastics to be utilized in EAF.
	Rubber tires	
	Blend of polymer and fossil coke	

4.3 Slag formers

Slag plays an important role in Electric Arc Furnace operations as it absorbs impurities, protects the refractory lining of the furnace and acts as a barrier against molten steel reoxidation and thermal losses. There are two main sources of slag in the EAF: the residual oxides from the hydrogen reduced DRI that can be referred as autogenous slag and materials that are charged into the EAF that are referred as slag formers. In addition, small amount of slag is from the refractory material of the furnace. Slag formers are added to the EAF charge in order to adjust the slag volume and its chemical and physical properties such as its basicity and viscosity. Basicity is a highly important parameter as it greatly affects the dephosphorization of the liquid metal. Phosphorus itself is a harmful impurity in steel as it decreases toughness and ductility of the steel product. It is removed in EAF process by oxidating the phosphorus to P_2O_5 which then transfers to the slag phase. The removal is favoured under oxidizing conditions and high slag basicity [70], [84].

Heo and Park [85] investigated the effects of dephosphorization in EAF using DRI as a feedstock. Two reaction steps: melting and slag-metal reactions were observed. Thermodynamic behaviour of phosphorus, oxygen and

carbon were strongly associated with the ratio of DRI and scrap that were charged to the EAF in the investigated temperature of 1550 °C. A higher DRI content in the feed decreased the basicity and the stability of P_2O_5 in the slag phase. Thus, highlighting the proper basicity in order to improve the dephosphorization.

Kirschen et al. [86] reported various slag masses and basicity values on different charging mixtures of conventional carbon containing DRI and scrap in an industrial electric arc furnace. As expected, the total slag mass was higher for pure DRI as the total gangue content was higher. This resulted in the increased slag former consumption to compensate for the acidic SiO_2 present in the DRI. Overall, when a majority of DRI was charged instead of scrap, several changes was observed in the slag: higher content of CaO and SiO_2 and lower content of Al_2O_3 and MnO, the MgO remained close to its saturation value in both cases. Standard slag basicity (B2) was in the range of 1.8-2.1. However, lower B2 values resulting in lower slag amounts can improve the efficiency of FeO reduction by carbon injection in the EAF. Thus, the goal is to find a right balance between the required dephosphorization and the amount of iron that is lost to the slag as FeO.

To conclude, in order to reach the desired EAF operating conditions such as the basicity, slag formers are added along with the autogenous slag from the DRI. Mostly utilized slag formers are lime and dolomite that include oxides such as CaO and MgO. The amount of slag formers varies depending on the iron material and tie charge mix but also the specifications required for the steel product. But typically, the charged amount of slag formers is 23-35 kg per tonne of steel when only scrap is charged, and 27-60 kg per tonne of steel when only DRI is charged. The ratio of lime to dolomite varies also depending on the process specifications and availability and price of the materials but typically lime is used in greater extent [86]. Table 13 compares the average chemical composition of lime and dolomite. However, the chemical composition of these slag formers can vary based on where they are sourced from.

Table 13. Average chemical composition of Lime and Dolomite used in EAF [87], [73].

Compound	**Lime, wt.%**	**Dolomite, wt.%**
CaO	>90	80.21
CO_2	1.5	-
Al_2O_3	Trace	1.52
SiO_2	0.09	2.50
Fe_2O_3	Trace	0.15
MgO	1.66	15.50
CuO	Trace	0.07
MnO	Trace	0.02

4.4 Considerations in the EAF when utilizing DRI

As discussed earlier, the Electric Arc Furnace is selected as the melting furnace and refining step in the examined process. The DRI product is transported to downstream EAF process as HDRI in order to take advantage of the heat content in the material. Continuous feeding is usually employed, when more than 25% of DRI is fed into the EAF, otherwise bucket charging may be employed [88]. In the EAF process, scrap can be added as an additional iron bearing raw material along with slag formers that allow the refining of the metal. At the EAF process carbon is injected to achieve the desired carburization of the liquid steel product.

At this moment it must be remembered that the on an industrial scale the demonstrated and mature direct reduction process followed by EAF is conducted in a reducing atmosphere containing both carbon monoxide and hydrogen. This results in the fact that the DRI product has a carbon content of 2-4 wt.%. However, when pure hydrogen is used as a reducing agent the resulting carburization is close to 0 wt.%. This raises a concern, among other things, the following: how it affects the energy consumption and produced slag volume and also if the beneficial slag foaming practise can be conducted [27].

Nuber et al. [89] and Hornby [90] addresses some of these issues and states that DRI/HBI with 0% carburization can be used in EAF with equal or superior technical and economic results by applying few changes to the operating procedure. Slag foaming practise can be carried out by proper injection of carbon and oxygen into the melt. When a majority of the EAF's feed material is DRI, a large hot heel is required to be left in the furnace in order to ensure proper melting and to avoid "iceberg" formation in the furnace. Also, these sources refer to a Circored plant in Trinidad that processed 0% C DRI in 2000-2001 with the result that phosphorus removal was good and sulphur removal behaviour was normal.

However, there are still downsides and challenges yet to be solved in using DRI with 0 wt.% carburization in the EAF process. If carbon is present in the material, part of it is consumed in the reaction with FeO in the slag phase and the excess carbon is burned thus providing chemical energy into the EAF and lowering the electricity consumption. So, carbon free DRI leads to higher FeO slag volume, and it is clear that carbon must be introduced to the EAF system in some other form. [88]. In addition, Ahmed et al. reported a higher liquidus temperature associated with using carbon free DRI which could lead to decreased productivity in the EAF. Understanding the effects of carbon free DRI will increase as the pilot trials are further conducted and standard operating procedures will develop.

In addition, to improve the overall sustainability of the process, a few remarks can be made. First, the natural gas burners that are typically used in some extent in the industrials EAF cause carbon dioxide emissions due to the burning of hydrocarbons. DevH2forEaf is a project that aims to develop a burner that is able to work with any kind of mixture of hydrogen and natural gas. According to the project, if 10% of the NG in the Europe is substituted with hydrogen, it would reduce the CO_2 emission by the steel sector by 100 000 tons/year [91], [92]. Thus, when the trend seems to be the transition towards more EAF based steelmaking, the use of hydrogen burners in the furnaces should be increased.

Secondly, even though the scope of this thesis does not include the secondary metallurgy. The closely related processes to the EAF such as ladle drying and preheating should be also considered when examining the sustainability of the H_2-DRI-EAF steelmaking process. Echterhof [93] states that the energy consumption of ladle drying and preheating is typically in the range of 10-25 kWh/tls and in practise is done by utilizing natural gas. Thus, for the German steel industry alone, the ladle preheating and drying step would emit around 140 000 tons of CO_2 per year.

EXPERIMENTAL PART

5 Research materials and methods

The applied part of this research focused on designing and building a simulation flowsheet of the H_2-DRI-EAF process using Metso's HSC Sim Flowsheet Module with HSC Chemistry 10. Currently, the HSC Chemistry software has 24 calculation modules that are connected to 12 integrated databases. HSC Sim Module allows the user to design a simulation flowsheet and to simulate for example various mineral processing, hydrometallurgical or pyrometallurgical unit processes. The calculations are based on general principles of chemistry and physics such as chemical equilibrium, material and energy balance calculations, as well as metallurgical databases developed by Metso. The simulation software supports both steady state and dynamic simulations. [4]

A process model was developed using the results from the literature review and especially the current commercial processes that are discussed in chapter 3.5. Briefly stated, the design proceeded by first drawing the units and then connecting the streams between them. Then input and output compounds and amounts were set followed by setting the elemental distributions and controls. Several rounds of revisions were made in order for the simulation model to be accurate.

The thesis examines the effects of raw materials by simulating nine different design scenarios. Both the quality of the iron ore pellets, and the ratio of scrap is varied in order to gain a better understanding on the effects of these variables to the process conditions and the end-product. The aim is to be able to analyse how these variables affect the energy consumption, slag volume and the final liquid steel composition. The investigated design scenarios hereinafter referred also to as 'cases' are presented on Table 14. Case 2A, which primarily uses typical DR-grade iron ore pellets and to a lesser extent steel scrap, is regarded as the base case. The steel scrap in the base case (20% of the charge) could be only internal scrap and not sourced from elsewhere. Whiles, the case with 80% scrap simulates a scrap based EAF with DRI used for dilution of tramp elements. All consumption and volumetric results are normalized to ton of liquid steel produced.

Table 14. The design scenarios of the raw materials used in the simulation of the H_2-DRI-EAF process.

	A. 20% scrap equivalent[1]	**B. 50% scrap equivalent[1]**	**C. 80% scrap equivalent[1]**
1. Low grade IO pellet 65.1 wt.% tot. Fe 7 wt.% Gangue	1A	1B	1C
2. Medium grade IO pellet 67.2 wt.% tot. Fe 4 wt.% Gangue	2A	2B	2C
3. High grade IO pellet 68.2 wt.% tot. Fe 2.5 wt.% Gangue	3A	3B	3C

[1] Exact recipe might differ as pellet consumption between qualities is calculated so that the metallic iron remains a constant that is achieved with BF-grade pellets.

These design cases were chosen because, as previously discussed, varying amount of steel scrap are often used in the industry, and it is important to study the joint effect of the ratio of DRI and steel scrap used in the process. In addition, the current public simulation studies do not consider the usage and the amount of steel scrap in the process chain [34], [94].

6 Simulation flowsheet

This chapter begins by introduction of the flowsheet that was simulated in this thesis. This is followed by an in-depth look at the simulation conditions for the shaft furnace and the electric arc furnace. Supplementary material including all of the assumptions is provided in the appendices.

6.1 Process description

A schematic of a process design for the investigated H_2-DRI-EAF process is presented in Figure 7. The hydrogen introduced to the system is from electrolyser units or from hydrogen storage that can be located at the production site, or it can be sourced over-the-fence. The simulation of the electrolysis is not included in the scope of this thesis. The hydrogen is heated by means of electrical heater in the 'Hydrogen Heater' unit and is fed to the middle of shaft furnace ('Shaft Furnace') where it rises upward in the furnace and meets the iron oxide material counter-currently. The reacted gas ('Vapour') consists of excess hydrogen and water vapour formed in the reaction. The iron oxide pellets are fed from the top of the shaft at ambient temperature ('Io Pellets In').

The reduced iron oxide pellets referred to in the flow sheet as 'HDRI' is discharged from the bottom of the shaft furnace. In practise in the transportation of DRI there is always some degree of cooling that is simulated with the 'Transportation Heat Losses' unit. The unit is a simple representation of the cooling that occurs in the transportation, thus the chemical composition of the DRI remains constant so no oxidation is assumed to occur. The DRI material that enters the downstream electric arc furnace is referred to as 'HDRI to EAF'.

The direct reduced iron is fed into the EAF along with steel scrap, slag formers, infiltrated air, oxygen and natural gas burner off gas. In addition, the simulation flowsheet incorporates streams 'Electrodes' and 'Refractories' to simulate the actual wear of the graphite electrodes and the refractory lining of the furnace. The outputs material streams are 'EAF Dust', 'EAF Off Gas', 'Slag' and 'Liquid Steel'. Two energy flows 'EAF Electrical Energy' and 'EAF Heat Losses' represents the amount of electrical energy that must be supplied to the furnace and on the other hand the significant heat losses incurred during the process.

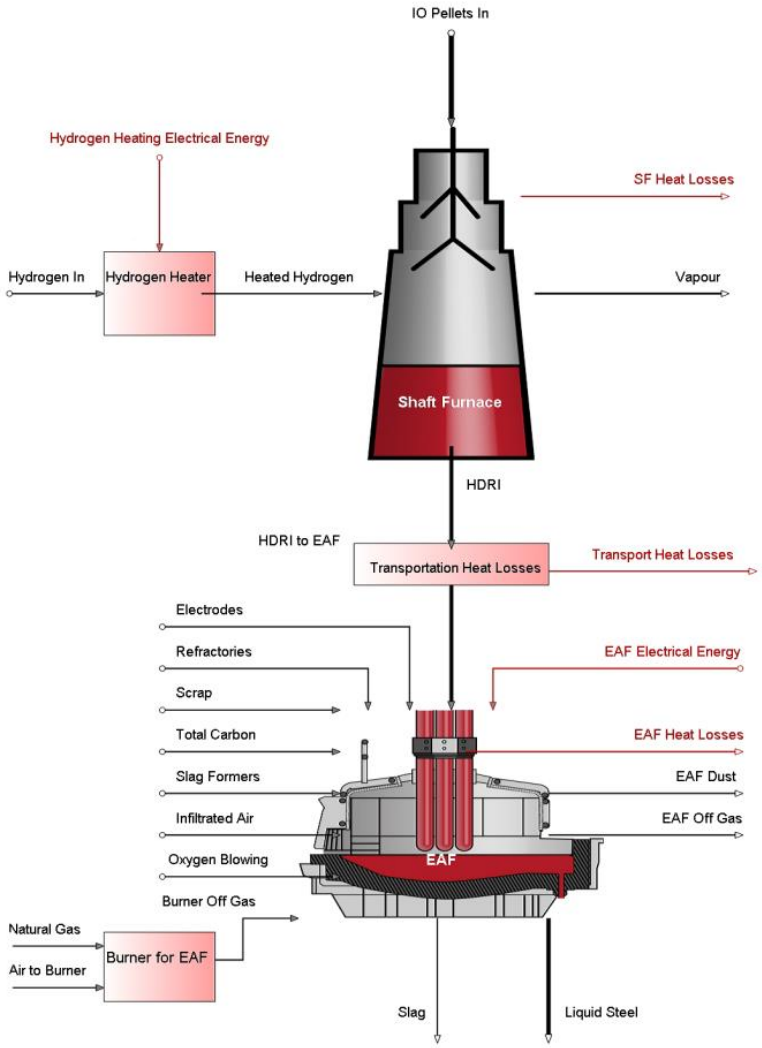

Figure 7. The simulated process: hydrogen-based shaft furnace followed by electric arc furnace melting of the produced DRI and steel scrap.

6.2 Simulation of shaft furnace

The shaft furnace was simulated as a distribution (pyro) unit in the HSC Sim Flowsheet Module. The feedstocks for the unit are iron ore pellets and pre-heated hydrogen. The furnace produces hot direct reduced iron and vapour that exits the shaft furnace. The most notable operating parameters of the shaft furnace process are the metallisation achieved and the heat balance of the process that is dictated by the reducing gas volume flow, temperature, recycling ratio and the heat losses.

Metallisation is the quantitative measure of the extent of the reduction of iron oxides that occurs in the shaft furnace. The metallisation for the medium grade IO-pellets is set to be 94% that is thought to be a common metallization

degree according to references in the literature [34], [75], [95]. However, as discussed previously, the metallisation is not constant but rather varies depending on, among other factors, the quality of the IO-pellets used. The metallisation for the BF-grade IO-pellets was set to 93%, while for the high-quality DR-grade IO-pellets were set a higher metallisation degree of 94,75% [40]. The chemical composition of the examined pellet grades is given in Appendix B.

The reducing gas was preheated to 900 °C and excess hydrogen was fed into the shaft furnace in order to make the process technically feasible from a thermodynamic standpoint. In order to achieve a gas oxidization degree (GOD) that is lower than 0.3 and to ensure that the top gas temperature is within a sensible range, a lambda ratio of 3.5 is used in the process model. This means that for example for the base case (2A), 1715 Nm^3 (76 kmol) of hydrogen has to be supplied to the shaft of which 490 Nm^3 (22 kmol) is consumed in the reduction of iron oxides and 1 225 Nm^3 (54 kmol) is excess hydrogen gas that can be recirculated back into the process. The circulation of the top gas is outside of the scope of the process model, as successful modelling of the recycled reducing gas requires a more in-depth knowledge of the shaft furnace and gas recycling system. However, Tenova's Energiron process scheme consists of a top gas scrubber unit and a water vapour condenser unit after which the clean gas is re-heated and recirculated back into the module, along with fresh gas [96].

The heat balance of the shaft furnace process is greatly affected by heat losses that occurs from the shaft furnace's walls. In the simulation flowsheet a heat loss value of 40 kWh/t steel was selected as it was discussed to be a suggested value by SSAB as reported in Andersson's doctoral thesis [95]. The temperature of the DRI that comes out of the shaft furnace was set to 725 °C that is an approximately 100 °C lower than the temperature of a HDRI that is obtained from the conventional natural gas reduction that is an exothermic process [96], [97].

Transportation of the DRI to the downstream EAF process causes the DRI to cool down. When simulating the hot DRI feed to EAF the 'Transportation Heat Losses' unit output temperature of the DRI is set to 600 °C. The rationale for this temperature was the Hotlink system that Midrex provides which aims to lower the energy consumption in the EAF as the hot DRI does not have to be heated up again. Downside to the Hotlink system is that the shaft furnace must be located at a maximum distance of 40 meters from the EAF which in turn can increase the investment cost of the steel mill. [54], [68], [98]. Thus, the 'Heat Losses' unit makes it possible to also investigate the scenario where ambient temperature hot briquetted iron material is fed into the EAF.

In practise the successful simulation of a process unit requires some controls to be set in the HSC program. This ensures that the energy and heat balances are achieved and that the model represents the designed scenario. Controls behave like a real process control: e.g., the user can assign a target value for a process unit temperature and regulate the temperature by changing the amount of fuel fed into the unit. In this thesis work, all of the controls are calculated by the tangential (fast) method that solves the controls by using modified tangent method [4]. The most important controls used in the simulation of the shaft furnace process are shown in Table 15. The simulation parameters for the simulation of the shaft furnace are given in Appendix D.

Table 15. Controllers for HSC simulation of hydrogen based DRI shaft furnace process.

Unit name	Measured	Controls
Hydrogen Heater	Heat balance.	Input electricity flow amount.
Shaft Furnace	Heat balance.	Vapour output temperature.
	Reducing gas to reach λ = 3.5.	Input hydrogen amount.
	Produced liquid steel in EAF to reach 1 ton.[1]	Iron ore pellet feed amount.[1]
	To produce equivalent mass of metallic Fe as with the BF-grade pellet.[2]	Iron ore pellet feed amount.[2]
Transportation Heat Losses	Heat balance.	Output heat loss energy flow.

[1] Applicable to cases 1A, 1B, 1C
[2] Applicable to cases 2A, 2B, 2C, 3A, 3B, 3C

By utilizing the best available data from the literature, carefully considered assumption, and the controls presented in Table 15, the modelling of the shaft furnace was successful without errors. In addition, with all the controls converging correctly in the Sim Model Convergence Monitor, both mass and energy balance were set as the monitoring criterion with a tolerance of 0.1%. The equations for the mass balance error and the enthalpy balance error are given in equations (19) and (20), respectively [4].

$$MBE - \% = \left(\frac{Total\ mass\ in - Total\ mass\ out}{Total\ mass\ in}\right) * 100\% \quad (19)$$

$$EBE - \% = \left(\frac{Total\ enthalpy\ in - Total\ enthalpy\ out}{Total\ enthalpy\ in}\right) * 100\% \quad (20)$$

6.3 Simulation of electric arc furnace

The electric arc furnace was also simulated as a distribution (pyro) unit in the HSC Sim Flowsheet Module. As mentioned, the EAF is operated batchwise but due to the restrictions posed by the HSC simulation programme, the flowsheet is built to showcase the consumption values to produce 1 ton of liquid steel. Thus, the simulation model takes no stand on the various refining stages (bore-in, main melting, meltdown, refining, heating) that occurs at specific time with their own operating procedures. The simulation of the EAF does not specify whether AC or DC furnace is used and what is the specific capacity of the furnace. In addition, the model does not try to simulate the hot heel practise which has been reported on being especially beneficial for high charges of DRI [99], [100].

The iron bearing feedstocks for the unit are direct reduced iron and steel scrap. The model does not specify the method or the time of charging the materials. In the study, three different DRI to scrap ratios are simulated. Steel scrap is charged at ambient temperature. In cases where blast furnace grade pellets are used, the amount of scrap is controlled by the target recipe. When DR-grade or high quality DR-grade pellets are used, the amount of scrap is controlled so that 1 ton of steel is produced in the system (see Table 15 and Table 16). The furnace produces liquid steel and a slag phase that are tapped out of the furnace at the temperatures of 1600 °C and 1650 °C, respectively.

As discussed in chapter 4.3, the basicity of the slag is an important parameter to optimize the dephosphorization and to ensure that the EAF process works properly with a long campaign life. The target slag basicity B2 as defined in equation (8) is set to 2.1 in all of the simulated cases as it ensures great phosphorus removal and is a value that industrial EAFs are operated at [86]. The basicity of the slag is increased by the addition of slag formers consisting of lime and dolomite. The chemical composition of the slag formers assumed in this study is given in Appendix E.

The practical modelling of the EAF requires a lot of thermodynamical knowledge in order to assign the correct distribution factors of different elements present in the raw material mix. Elements are distributed to liquid steel, slag, off gas or dust with various distribution ratios. The distributions of different elements were mainly gathered from suitable best available literature references [101], [102] and assumptions that are backed up by different analysis of metal and slag phase in an industrial steel mill. For instance, in the process model, all of the zinc fed into the EAF was assumed to be burned

off and thus end up in the dust stream. A more rigorous depiction of the elemental distributions are given in Appendix F.

In order to study the energy consumption of the electric arc furnace, a proper understanding of a typical EAF energy balance is required. Approximately half of the energy in the EAF is supplied by the electric arcs and the rest provided by various chemical reactions. Thus, the amount of carbon carriers, natural gas burners and the amount of oxygen blowing conducted in a furnace was set and benchmarked carefully according to data from industrial furnaces in order to be able to make best estimates of the change in the energy consumption in the simulated cases. All of the assumptions used in the modelling of the EAF is given in Appendix E.

In order to successfully simulate the EAF and to be able to create a coherent model that can be seamlessly tailored to different scenarios, controls were set in the unit model. The most important controls used in the simulation of the electric arc furnace are shown in Table 16. Rest of the controls in the model were set in order to assign the correct distribution factors for the elements. A total of 21 controls were set in the modelling of the EAF.

Table 16. Controllers for HSC simulation of electric arc furnace.

Unit name	Measured	Controls
Burner For EAF	Heat balance.	Output off gas temperature.
EAF	Scrap ratio (to reach 20%, 50% or 80% depending on the case to be simulated).[1]	Input scrap amount.[1]
	To produce 1 ton of liquid steel in the EAF.[2]	Input scrap amount.[2]
	Heat balance.	Input electricity flow amount.
	Slag basicity (B2) to reach 2.1.	Input slag formers amount.
	Carburization to reach 0.03 wt.%.	Carbon elemental distribution to metal rest is distributed to off gas and dust
	FeO in the slag to reach 30 wt.%.	Iron elemental distribution to slag rest is distributed to metal and dust

[1] Applicable to cases 1A, 1B, 1C
[2] Applicable to cases 2A, 2B, 2C, 3A, 3B, 3C

7 Results and discussion

In this section, the results of the applied part of the study are presented. First, the general results of the simulation flowsheet are presented. This is followed by chapters that discuss the effects of raw materials on different process conditions. Also, the estimated energy consumption and CO_2 emission figures are presented and discussed. In addition, the model does not only generate the discussed main results but also other results that are not so relevant to this study: e.g., the per TLS produced dust amount in the process which is based on the EAF zinc balance. All the results have been compiled into Appendix G.

7.1 Effects of raw materials/Scenario analysis

The simulation flowsheet was built with HSC 10 software using pyro units. Nine different scenarios were investigated: three different IO pellet qualities and three different ratios of DRI to steel scrap. The DRI was assumed to be directly transported from the shaft furnace to the electric arc furnace in order to take advantage of the heat content that is present in the DRI material. The main results from the simulation study are presented in Table 17. More details about the results are discussed in the following chapters.

Table 17. Relationship between variation of process parameters and process performance data estimated by the simulation flowsheet.

	Increasing the purity of the iron oxide pellet[1]		**Increasing the ratio of scrap to DRI in the charge[2]**	
Iron ore pellet consumption	↘	-8 %	↓	-77 %
Hydrogen consumption	→	-1 %	↓	-77 %
Metallisation in the shaft furnace	↑	2 %	→	0 %
EAF energy consumption	↘	-17 %	↘	-15 %
Tap-to-tap time	→	0 %	↘	-17 %
Slag Mass	↓	-71 %	↘	-22 %
Slag Former Consumption	↓	-75 %	↘	-23 %
Produced CO_2 (Direct)	→	0 %	↘	-28 %
Copper content in steel	↘	-15 %	↑	315 %

[1] Relative change from 3A compared to 1A
[2] Relative change from 2C compared to 2A

The benefits of increasing the purity of the iron oxide pellet can be clearly seen from Table 17. When the process uses high quality DR-grade io pellets instead of blast furnace grade pellets several advantages can be leveraged. The IO consumption decreases as less gangue material is moved around in the process. The little difference in hydrogen consumption is due to the better metallisation that is assumed to be realised with higher grade of pellets. The energy consumption in the electric arc furnace is greatly reduced together with the mass of produced slag. Also, on the other hand, the use of slag formers decreases but no changes were reported in the direct CO_2 emissions. With a higher-grade iron ore pellet the copper content in the steel decreased.

Also, from Table 17 the benefits of increasing the charged amount of scrap, thus making the process behave more like a traditional scrap based EAF, can clearly be seen. The iron ore pellet and hydrogen consumption decrease as more of the iron in the steel originates from the scrap that requires no reduction like the DRI. The energy consumption is decreased together with tap-to-tap time as steel scrap produces less slag and the melting is less energy intensive, partly due to the increased use of natural gas burners. Produced slag and consumption of slag formers are decreased among the direct CO_2 emissions. But on the contrary, the copper content in the steel product increases as it is present in the scrap material.

7.1.1 Effects of raw materials in produced metallurgical slag

As discussed before, the hypothesis is that the less pure the iron bearing raw materials are, the more metallurgical slag is formed in the melting of stage of the raw materials. And on the other hand, when the mass of acidic compounds in the feed increases, it requires more slag formers to maintain a proper slag basicity level in the furnace. The produced slag masses and the consumed slag former masses of the different design scenarios are presented in Table 18.

Table 18. The produced slag (upper value) and slag former (lower value) consumption in the EAF estimated by the flowsheet model.

	A. 20% scrap[1]	**B. 50% scrap[1]**	**C. 80% scrap[1]**
1. BF-grade pellet	304 kg/tls 90 kg/tls	220 kg/tls 64 kg/tls	143 kg/tls 40 kg/tls
2. DR-grade pellet	134 kg/tls 35 kg/tls	120 kg/tls 31 kg/tls	106 kg/tls 27 kg/tls
3. High quality DR-grade pellet	88 kg/tls 22 kg/tls	91 kg/tls 23 kg/tls	94 kg/tls 24 kg/tls

[1] Exact recipe might differ as pellet consumption between qualities is calculated so that the metallic iron remains a constant that is achieved with BF-grade pellets.

As seen from Table 18, the blast furnace grade pellet with 20% steel scrap produced the most slag (304 kg/tls). This is due to the pellet containing most impurities and especially acidic impurities that require more slag formers to be used in order to achieve the required basicity (B2). The slag volume in the 1A case greatly exceeds the volume that is produced in a typical EAF process. The large amount of slag increases the energy consumption in the process, and it has to treated in a proper manner, thus the blast furnace grade overall poses an issue to the process. In addition, the slag formers consumption increases, thus increasing the OPEX of the EAF melting. When the amount of scrap is increased as in cases 1B, 1C the produced slag decreases by 28% and 53%, respectively compared to the base case. When comparing the ratios of slag formers to produced slag, it can be observed that the ratio is at its highest when using BF-grade pellets and varies more when comparing BF-grade to DR-grade rather than DR-grade to high quality DR-grade pellets.

When the purity of the pellet increases, the amount of slag and slag formers decreases in all of the examined scrap ratios. With 20% scrap in the charge, a 127% increase in slag is estimated with BF-grade pellets and a 34% decrease in the slag is estimated with high quality DR-grade pellets when comparing both to DR-grade pellets. Generally, when the ratio of scrap to DRI increases, the slag mass decreases as the steel scrap is purer than BF-grade and DR-grade purity. However, for the high-quality DR-grade, we observe that the slag mass increases slightly when the amount of scrap increases. Whether this is actually observed in a real process depends on the purity of the scrap. But it can be stated that the ore base metallics feed material can be purer than some types of ferrous scrap. The slag formers to slag mass ratios remains almost the same when comparing 20% to 50% scrap recipes but varies slightly when comparing 50% to 80% scrap recipes.

In the simulation model, the slag composition is calculated from the mass balance and the elemental distributions that are set in the model. The chemical composition of the simulated slag phase compared to typical industrial values are given in Table 19.

Table 19. Chemical composition of the slag phase produced in the EAF [86], [103], [104], [105].

Compound	Simulated	Industrial reference
CaO, wt.%	32–36	27–34
FeO, wt.%	30	29–48
SiO_2, wt.%	15–17	11–18
MgO, wt.%	9–11	4.5–9.3
Al_2O_3, wt.%	2.6–5.1	3.8–7.7
MnO, wt.%	1.3–6.0	1.0–7.6
Cr_2O_3, wt.%	0.1–1.5	0.2–2.8
TiO_2, wt.%	0.4–1.6	0.3–1.2
P_2O_5, wt.%	0.6–0.8	0.1–0.6

It can be generally stated from Table 19 that the values calculated by the simulation correspond well with the slag composition values reported in the industry. Also, it can be seen that the industrial reference values can vary a lot for example for FeO and MnO content varies based on the feedstock and the standard operating procedure. MgO is an important slag component due to its influence on the consumption of the EAF refractory lining.

The content of the MgO should be close to its saturation limit. In practise, the saturation of MgO depends on, among other things, the temperature and the overall chemical composition of the slag phase. According to MgO saturation data by Kirchen [100] with 5% Al2O3 at 1600°C, we can state that for example for the base case (2A) the slag produced in the system is close to its MgO saturation, so the process is not too harsh on the refractory lining of the furnace. Thus, the assumed consumption of the refractory lining corresponds with the slag saturation aspect.

In the future, when the standard operating procedures are developed for 0 C wt.% DRI, more knowledge of the slag chemistry within different scrap charges will be gathered. Thus, different optimal practises for the EAF will be used in the steelmaking plants to produce the desired steel grades from economically viable feedstocks.

7.1.2 Effects of raw materials in the product

As discussed previously, no industrial EAFs are operated with hydrogen reduced DRI that does not contain any carbon. As a result, no indepth knowledge of elemental distrubutions or metallic yields are available in the literature. Thus, the results conserning the purity of the produced steel or the yields calculated can be only considered as indicative.

The calculated total iron yields of the process are in the range of 93.0-97.6% which can be considered to be quite high values. The lowest yields are obtained when the blast furnace grade pellets are used in steelmaking. Whileas the highest iron yields are from the charges where the pellet quality is good and 80% of steel scrap is used in the process. Thus, the general trend is reasonable, as blast furnace grade pellets were anticipated to lead to lower steel yields in the process chain. Figure 8 presents a sankey diagram, showing input and output streams of iron.

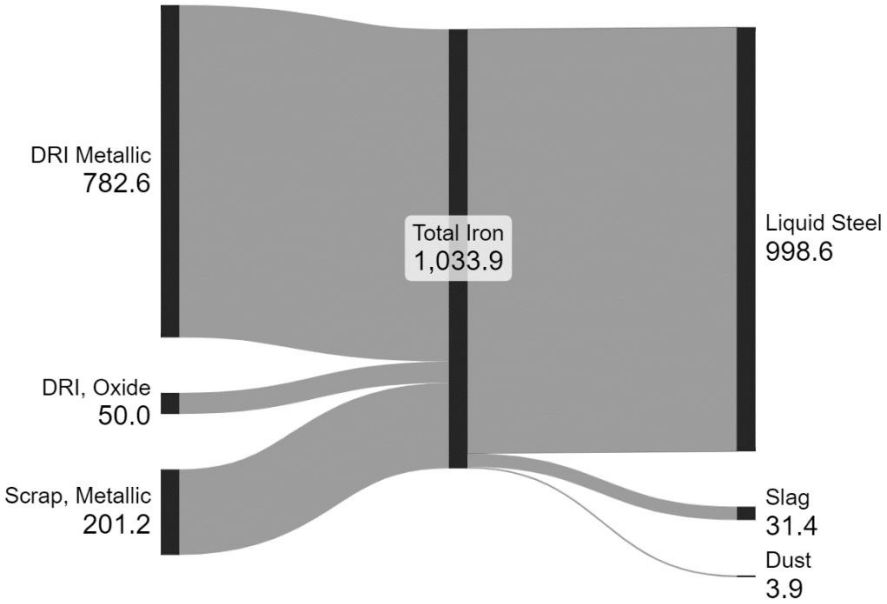

Figure 8. Sankey diagram of the iron balance for the base case (2A) where EAF was charged with DR-grade pellets and approximately 20% scrap.

As can be seen from Figure 8 where DR-grade iron ore pellets are used among 20% scrap, the iron yield for the process is 96.6%. Some of the iron that is in the form of FeO gets reduced to metallic iron in the EAF with the addition of carbon. While a notable amount of iron ends up in the slag phase according to the set control target. A minor amount of the iron in the input ends up in dust.

The introduction of ore based metallic iron into the EAF feed has the positive effect of diluting the scrap residual contents. Especially copper raises concerns among steel producers but also other residual elements such as tin, nickel and molybdenum should be considered when producing certain steel grades. The amount of copper and the sum of the mentioned residual elements and how they can be diluted with the addition of DRI are shown on Table 20.

Table 20. Comparison on the copper and residual elements content on the simulated steel.

	A. 20% scrap[2]	**B. 50% scrap[2]**	**C. 80% scrap[2]**
1. BF-grade pellet	Cu: 607 ppm Resid.: 888 ppm[1]	Cu: 1447 ppm Resid.: 2115 ppm[1]	Cu: 2211 ppm Resid.: 3233 ppm[1]
2. DR-grade pellet	Cu: 528 ppm Resid.: 772 ppm[1]	Cu: 1400 ppm Resid.: 2047 ppm[1]	Cu: 2194 ppm Resid.: 3207 ppm[1]
3. High quality DR-grade pellet	Cu: 517 ppm Resid.: 757 ppm[1]	Cu: 1393 ppm Resid.: 2037 ppm[1]	Cu: 2191 ppm Resid.: 3203 ppm[1]

[1] Residuals, sum of Cu, Sn, Ni, Mo is given.

[2] Exact recipe might differ as pellet consumption between qualities is calculated so that the metallic iron remains a constant that is achieved with BF-grade pellets.

The scrap fed into the EAF had a copper content of 0.25 wt.% which is a typical value for scrap material. All of the copper fed was assumed to go to the metal phase. The tolerable amount of copper depends on the steel grade that is being produced: rebar, commercial and drawing steel grade has a maximum allowable copper content of 0.4, 0.1 and 0.06 wt.%, respectively [106]. So, from Table 20 it can be observed that with the right amount of dilution by DRI, all of the mentioned copper tolerances could be met in order to achieve the product with desired qualities. Therefore, the need for dilution can be highlighted, as according to Jeremy Jones in world steel association open forum 2030, it is expected that in 2050, there will be an average 0.5 wt.% copper in steel scrap [107]. The other residual elements exhibit the same dilution pattern as copper with different maximum allowable tolerances depending on the steel grade.

7.1.3 Effects of raw materials in energy consumption

As with most process concepts related to the green transition, the production of steel with the more sustainable H_2-DRI-EAF process, compared to BF-BOF process, requires more electricity to power the process as the transition from the fossil fuels takes place and results in higher electricity consumption. This raises a concern regarding whether the energy consumption of the process is too large that makes the process economically extremely unprofitable. When a typical direct reduction iron ore pellet grade is used with 20% scrap, the model estimates an energy consumption of 3.2 MWh for the H_2-DRI-EAF process chain. The specific energy consumption (SEC) for the base case (2A) has been compared with the results available from the literature, shown in Figure 9.

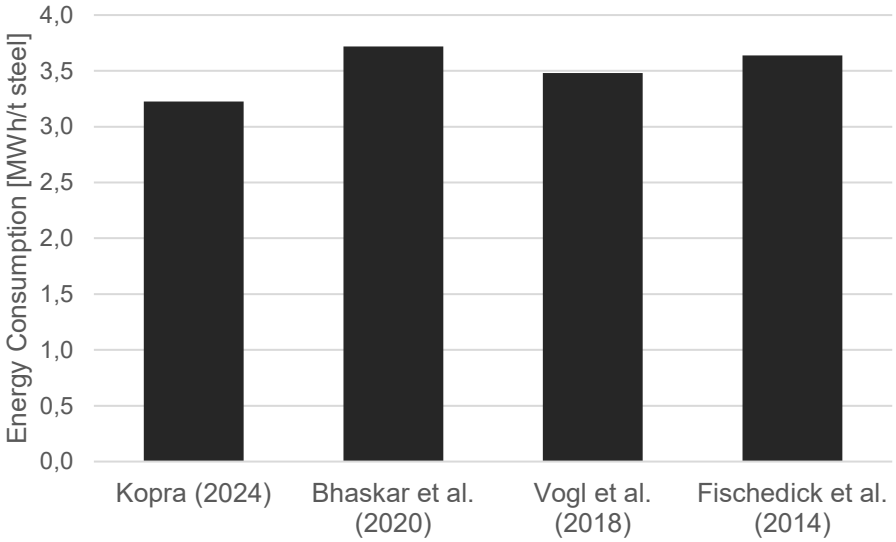

Figure 9. Comparison of energy demand for the H_2-DRI-EAF process with literature [34], [94], [108].

From Figure 9, we can see that the conducted study estimates the energy consumption of the process to align with other studies but to be somewhat lower. The difference between the estimated energy consumption arises from different process concepts and assumptions such as efficiencies used in the calculations. For example, Bhaskar et al. [34] and Vogl et al. [94] considers the usage of IO pellet heater to heat the preheat the pellets and the feedstock is only DRI without the usage of steel scrap. The study by Fischedick et al. [108] does not specify all of the assumptions in the model such as the temperature of the DRI that is fed into the EAF. In addition, the present model uses natural gas burners in the EAF to provide chemical energy which in turn lowers the electricity consumption of the furnace.

In this study, the energy consumption comprises from the electrolysis of water, the preheating of the reducing gas and the electricity consumed in the electric arc furnace. As discussed in the chapter 3.2, the electrolysers consume a lot of electricity, so it is reasonable to assume that the majority of the energy consumption is from the hydrogen production when large amounts of DRI is used in the process. However, it must be noted that the model does not include the recycling of the reducing gas and the hydrogen heater efficiency is assumed based on another published model and data provided by an equipment manufacturer [34], [66]. The energy consumption estimated by the model of the different design scenarios is presented in Figure 10.

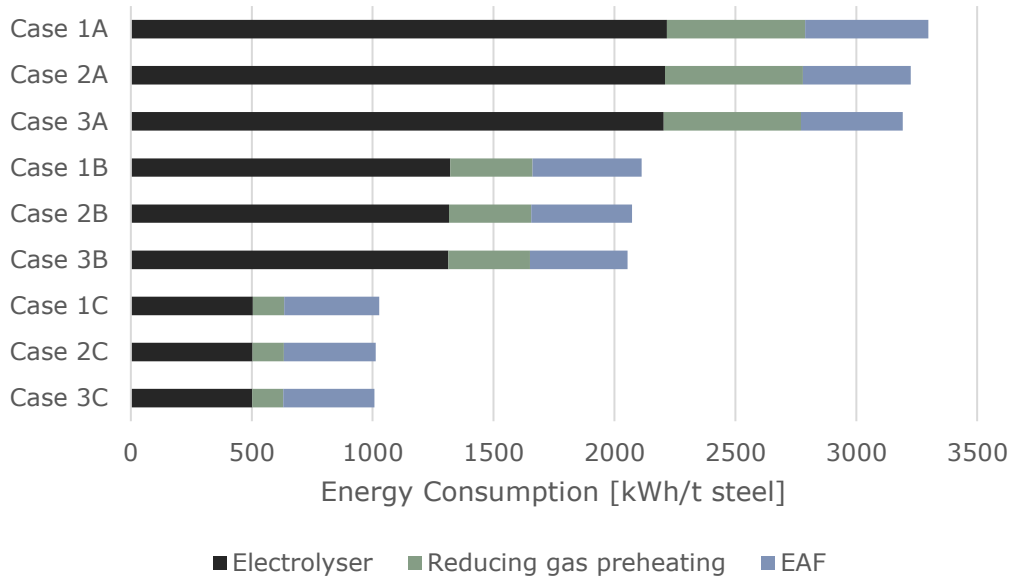

Figure 10. The energy consumption of the different design scenarios.

As can be seen from the Figure 10, most of the energy is consumed in electrolysers when using large amounts of DRI. The largest differences in the energy consumption rise from the charged amount of steel scrap. The largest energy consumption is reported in cases 1A, 2A, 3A which uses only approximately 20% of steel scrap as charge material. This is due to the fact that the DRI production requires hydrogen to be produced via electrolysis and the preheating of the hydrogen both of which are energy intensive. Also, the DRI requires more energy due to the larger slag volume that scrap in the EAF compared to the steel scrap. The energy consumption figures estimated in the EAF are shown in Table 21.

Table 21. The energy consumption in EAF of the different design scenarios

	A. 20% scrap[1]	**B. 50% scrap[1]**	**C. 80% scrap[1]**
1. BF-grade pellet	509 kWh/tls	451 kWh/tls	392 kWh/tls
2. DR-grade pellet	446 kWh/tls	417 kWh/tls	380 kWh/tls
3. High quality DR-grade pellet	421 kWh/tls	403 kWh/tls	376 kWh/tls

[1] Exact recipe might differ as pellet consumption between qualities is calculated so that the metallic iron remains a constant that is achieved with BF-grade pellets.

As can be observed from Figure 10 and Table 21 the quality of the pellet mainly affects the energy consumption in the EAF melting stage as the differences in the hydrogen consumption in the DRI process are relatively small.

A clear trend visible from the results is that the purer io pellet requires less energy in the EAF as it contains less components that end up in the slag phase. When approximately 20% scrap is used in the charge, the energy consumption increases by approximately 20% when comparing blast furnace grade pellets to high quality direct reduction pellets. The energy consumption is dependent also on the charging method for the DRI and the scrap which is beyond the scope of this study. Bucket charging versus continuous charging of the DRI might lead to significant changes in the energy consumption of the furnace. Also, according to SSAB [109], when cold DRI or HBI is used the energy consumption increases by approximately 20 kWh/tls for each 100°C decrease in the DRI charging temperature. Thus, if the furnace would be charged only with DRI the energy consumption changes between the hot DRI (600 °C) and ambient temperature sponge iron would be approximately 125 kWh/tls.

7.1.4 Effects of raw materials in CO_2 emissions (Scope 2)

Even though the term “green steel” or “fossil free steel” is often associated with the studied H_2-DRI-EAF process concept, it is still important to examine the true amount of carbon dioxide that the process generates. In this study, both the scope 1 emissions that the process produces directly and the scope 2 emissions that are indirect emissions from electricity are considered. The estimated CO_2 equivalent emissions including direct emissions and emissions caused by the consumed energy is presented in Figure 11. The figure is calculated based on Finland’s grid emission factor and a value of 85 gCO_2/kWh is considered in the calculations.

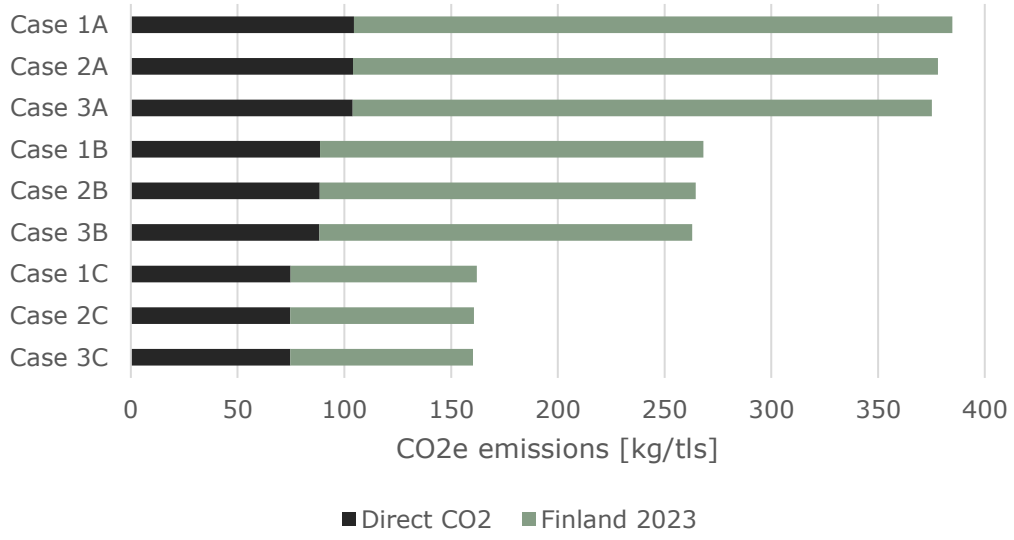

Figure 11. Comparison of CO_2e emissions of the design scenarios

From Figure 11 it can be observed that there are no significant changes in the direct emissions. These direct emissions originate from the addition of carbon materials in the EAF process. However, when more DRI is used, more carbon is assumed to be used in the process, thus resulting in larger amounts of carbon dioxide to be emitted. On the other hand, when the charge is based on scrap, less total carbon has to be supplied to the EAF. However, still some carbon is needed to carburize the charged amount of DRI and to ensure the slag foaming practise. Thus, is logical that no changes in the direct emissions are noticed when the recipe in the EAF is constant and only the pellet quality is altered.

As can be seen from the Figure 11, a majority of the carbon dioxide emissions are from the electricity consumed when Finnish grid emissions are used in the calculations. The differences in the indirect emissions are due to the changes in the energy consumption as discussed in the previous chapter. In order to understand the importance of the development of the electricity grid, it must be benchmarked against other locations. Table 22 compares the emissions caused from the base case (2A) with average grid emissions factors from Sweden, Finland, the European Union and the Unites States (contiguous). The respective emissions factors (yearly averages) of 25 gCO_2/kWh, 85 gCO_2/kWh, 251 gCO_2/kWh and 411 gCO_2/kWh are considered in the calculations.

Table 22. CO_2e emissions variation with countries when using DR-grade pellets and 20% of scrap (Case 2A).

	Base case CO_2e [kg/tls]	**Indirect emissions compared to Sweden**
Direct emissions	104	-
Sweden	81	1.0x
Finland	274	3.4x
EU (average) in 2022	809	10.0x
US (contiguous) in 2023	1325	16.4x

Table 22 clearly highlights that the overall carbon dioxide emissions of the process can vary by a significant amount based on the sourced energy. Thus, as of now the H_2-DRI-EAF process is not a “one size fits all” solution but the carbon intensity of the electricity grid must be carefully considered. The reduction of CO_2 emissions greatly depends on the electricity grid and in some locations, it might be more beneficial to utilize the natural gas-based process. The table also acts as a one explainer on why many of the projects discussed in chapter 2.4 are planned to be located in Sweden. It can be stated that the Swedish steel companies are the pioneers of hydrogen-based steelmaking, which is driven by their reasonably cheap electricity and green electricity grid [61].

Even though the carbon intensity of the process depends on the sourced electricity, the emissions can still be high compared to existing steelmaking operations. Previously, it has been discussed that currently the EAF is the less carbon intensive process followed by natural gas based DRI-EAF process and blast furnace – basic oxygen furnace process scheme. The estimated emissions of the hydrogen-based route are compared to the average emission by the existing processes in Figure 12. In Figure 12, Finland's 2023 average grid emission value is used in the calculation of the hydrogen-based route.

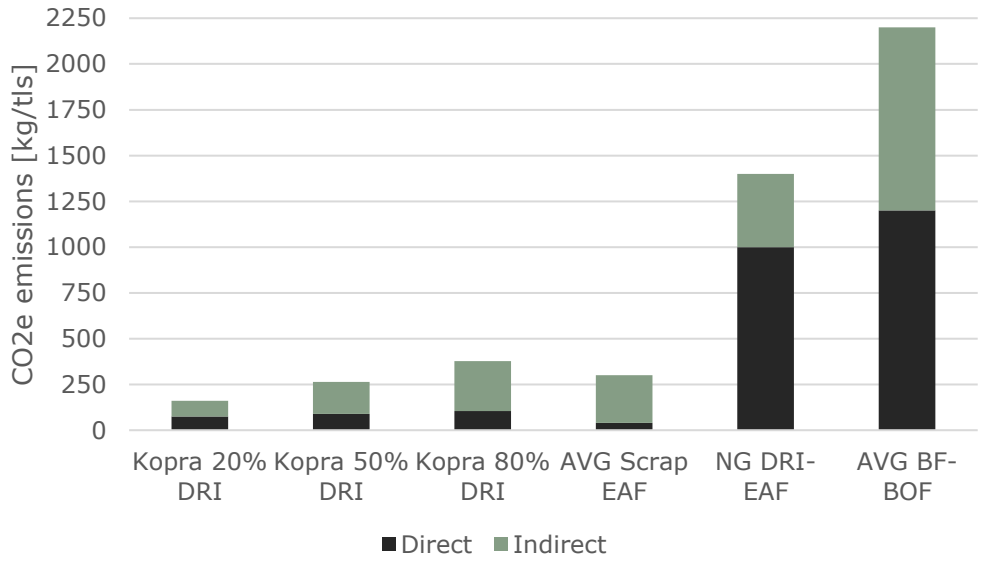

Figure 12. The comparison of CO_2e emissions based on process route [14].

As seen from Figure 12, the H_2-DRI-EAF process leads to emissions close to the existing scrap based electric arc furnace process. The model estimates that when 20% DRI is used, in Finland the emissions would be lower and on the other hand when 80% DRI is used the emissions would be a bit higher than the average EAF. As expected, the results show that the H_2-DRI-EAF process exhibits the same emission pattern as with EAF with most of the emissions being indirect emissions. However, the solely scrap based EAF has lower direct emissions due to the fact that less carbon has to be added to the system compared to charging with 0 wt.% C DRI.

The benefits of the hydrogen-based process can clearly be seen when comparing the H_2-DRI-EAF process with the existing natural gas DRI process and the BF-BOF process. The direct emissions are remarkably lower as well as the total emissions caused to produce one ton of steel. In Finland the H_2-DRI-EAF process allows for 71%-88% CO_2 emission reduction compared to NG-DRI and 82%-92% compared to BF-BOF, in Sweden the values are 86-93 and 91-95%. The model aligns with the potential CO_2 reduction up to 95% mentioned in chapter 3.3 when the direct emissions are set to zero.

8 Conclusions

This thesis has assessed the production of steel with the H_2-DRI-EAF process concept by utilizing only hydrogen as a reducing agent. The process concept is particularly interesting as it would allow for a drastic decrease in the carbon dioxide emissions of steelmaking and has thus generated multiple projects to target this outcome. The thesis examined the effect of iron ore pellet quality and the charged ratio of scrap in the process. Process simulation modelling the shaft furnace and electric arc furnace were implemented in HSC and nine scenarios were modelled with varying pellet qualities and scrap charges. It was noticed that the used HSC software is suitable for simple mass and energy balance base modelling of the process, but a more rigorous process model would require a more advanced software. The base case estimated an energy consumption of 3.2 MWh per ton of produced steel and 104 kg direct CO_2e emissions per ton of produced steel. Even though the study did not provide results regarding the operational expenses, it can be said that the feasibility of the process depends on fees imposed by regulation and the price of electricity as the process is powered by electricity. In addition, it is important to consider the differences in the price of the reductant and the sustainability of the electricity, when considering whether to utilize only hydrogen or some amount of natura gas in the direct reduction process.

The scenario analysis showed that it is beneficial for the process to utilize good-quality iron ore pellets instead of the examined blast furnace grade pellets due the increased energy consumption and slag mass produced when blast furnace pellets were implemented. Thus, indicating that if lower grade iron ore pellets are to be used, it would be better to pair the shaft furnace with a special electrical smelter or a blast furnace rather than an electric arc furnace. Also, the results indicated that the process benefits from heavy use of steel scrap, so it is beneficial to use scrap to the extent that is available in the production site. When the ratio of scrap is increased, less hydrogen is consumed in the shaft furnace and significant energy savings are observed in the downstream EAF process. Yet, as highlighted, steel scrap alone cannot supply enough iron bearing raw materials in order to meet the markers growing demand for steel. In addition, the anticipated increase in copper content in the steel scrap requires dilution with ore based metallics and for that purpose the hydrogen reduced DRI is the most environmentally friendly technology.

The examined process concept is still in its infancy on an industrial scale and thus the model and its assumptions would greatly benefit from more detailed information regarding the process conditions. For example, the 100% hydrogen reduction of iron oxide is proven on a pilot-scale but not on an industrial scale. It could cause problems such as the shaft furnace cooling and a lower degree of metallisation as the process is operated continuously. The recycling

of the reducing gas would also be beneficial for the process. Also, the downstream EAF melting has many uncertainties such as the melting behaviour of carbon free DRI and the iron yield that will be achieved. These questions will be answered as the bigger scale pilot testing progresses and the first hydrogen-based mills are commissioned. More research is also needed on more sustainable carbon containing materials and the hydrogen burners that has the potential to replace natural gas burners in the electric arc furnace.

In summary, the hydrogen based direct reduction followed by electric arc furnace process offers a significant chance to reduce carbon emissions in steelmaking. It is interesting to see how the projects regarding the H_2-DRI-EAF process concept evolves and whether the technical questions can be answered or if new ones are encountered. Also, it is interesting to see if steelmakers systematically choose DR-grade pellets and what will be the quality spread, and if blast furnace pellets are used in EAF or in some other furnace. Perhaps too much emphasis is given in the steelmaking industry to what could be done (hydrogen reduction) instead of which things could be implemented at this time, such as using more NG-based DRI and feeding it to a blast furnace, for instance. There is an urgency in combating the climate change and it is better to reduce emissions immediately rather than to wait for the perfect net-zero carbon dioxide process to be fully refined.

References

[1] International Energy Agency (IEA), “Iron and Steel Technology Roadmap - Towards more sustainable steelmaking,” Oct. 2020.

[2] K. Rechberger, A. Spanlang, A. Sasiain Conde, H. Wolfmeir, and C. Harris, “Green Hydrogen-Based Direct Reduction for Low-Carbon Steelmaking,” *steel research int.*, vol. 91, no. 11, May 2020, doi: 10.1002/srin.202000110.

[3] M. P. Smith, “Blast Furnace Ironmaking – A View on Future Developments,” *Procedia Engineering*, vol. 174, pp. 19–28, 2017, doi: 10.1016/j.proeng.2017.01.133.

[4] “HSC Chemistry,” Metso. Accessed: Mar. 18, 2024. [Online]. Available: https://www.metso.com/portfolio/hsc-chemistry/

[5] World Steel Association, *Steel Facts*. 2023. Accessed: Nov. 01, 2024. [Online]. Available: https://worldsteel.org/wp-content/uploads/worldsteel-book-final-2022-1.pdf

[6] “Iron & steel,” IEA. Accessed: Jan. 12, 2024. [Online]. Available: https://www.iea.org/energy-system/industry/steel

[7] United Nations, Department of Economic and Social Affairs, Population Division, “World Population Prospects 2022, Online Edition.” Accessed: Jan. 12, 2024. [Online]. Available: https://population.un.org/wpp/Download/Standard/MostUsed/

[8] “December 2023 crude steel production and 2023 global crude steel production totals,” worldsteel.org. Accessed: May 30, 2024. [Online]. Available: https://worldsteel.org/media/press-releases/2024/december-2023-crude-steel-production-and-2023-global-totals/

[9] R. Tang, “China’s steel industry and its impact on the United States: Issues for congress,” *Federal Publications*, Oct. 2010.

[10] S. K. Dutta and Y. B. Chokshi, *Basic Concepts of Iron and Steel Making*. Singapore: Springer Singapore, 2020. doi: 10.1007/978-981-15-2437-0.

[11] S. Seetharaman, A. McLean, R. I. L. Guthrie, and S. Sridhar, *Treatise on process metallurgy*. Amsterdam Waltham Paris: Elsevier, 2014.

[12] V. A. Shatlov, P. G. Netrebko, B. F. Marder, V. I. Bondarenko, V. V. Taranovskii, and O. L. Dan’shin, “Composition of ‘pig’ iron,” *Metallurgist*, vol. 16, no. 6, pp. 384–388, Jun. 1972, doi: 10.1007/BF00736743.

[13] IEA, “World Energy Outlook 2023.” [Online]. Available: https://www.iea.org/reports/world-energy-outlook-2023

[14] S. Nicholas and B. Soroush, “New from old: The Global Potential for More Scrap Steel Recycling,” IEEFA, Dec. 2021.

[15] SSAB, “SSAB Webinar: ‘Fossiilivapaa teräs ja ympäristöselosteet - kaksi tärkeää tekijää tulevaisuuden kestävän kehityksen työssä,’” Online, Apr. 2021.

[16] K. E. Daehn, A. Cabrera Serrenho, and J. M. Allwood, “How Will Copper Contamination Constrain Future Global Steel Recycling?,” *Environ. Sci. Technol.*, vol. 51, no. 11, Jun. 2017, doi: 10.1021/acs.est.7b00997.

[17] *Report from the commission to the European parliament and the council on the functioning of the European carbon market in 2021 pursuant to articles 10(5) and 21(2) of Directive 2003/87/EC (as amended by Directive 2009/29/EC and Directive (EU) 2018/410)*. 2022. Accessed: Jan. 19, 2024. [Online]. Available: https://eur-lex.europa.eu/legal-content/EN/TXT/?uri=COM:2022:516:FIN

[18] H. Muslemani, X. Liang, K. Kaesehage, F. Ascui, and J. Wilson, “Opportunities and challenges for decarbonizing steel production by creating markets for ‘green steel’ products,” *Journal of Cleaner Production*, vol. 315, Sep. 2021, doi: 10.1016/j.jclepro.2021.128127.

[19] M. Persson-Gulda, “H2 Green Steel - Building the world’s first large-scale green steel plant,” presented at the Green Steel World Expo, Essen, Germany, Apr. 04, 2023.

[20] M. Åhman *et al.*, *Hydrogen steelmaking for a low-carbon economy: A joint LU-SEI working paper for the HYBRIT project*. 2018.

[21] R. R. Wang, Y. Q. Zhao, A. Babich, D. Senk, and X. Y. Fan, “Hydrogen direct reduction (H-DR) in steel industry—An overview of challenges and opportunities,” *Journal of Cleaner Production*, vol. 329, Dec. 2021, doi: 10.1016/j.jclepro.2021.129797.

[22] M. Pei, “SSAB’s Transformation to a Fossil Free Steel Company with HYBRIT,” presented at the WSA Breakthrough Technology Conference, Abu Dhabi, Dec. 06, 2023.

[23] X. Zhang, K. Jiao, J. Zhang, and Z. Guo, “A review on low carbon emissions projects of steel industry in the World,” *Journal of Cleaner Production*, vol. 306, p. 127259, Jul. 2021, doi: 10.1016/j.jclepro.2021.127259.

[24] “SALCOS,” SALCOS®. Accessed: Feb. 13, 2024. [Online]. Available: https://salcos.salzgitter-ag.com/en/index.html

[25] Thyssenkrupp, “Climate-neutral steel - Our strategy,” thyssenkrupp. Accessed: Jan. 24, 2024. [Online]. Available: https://www.thyssenkrupp-steel.com/en/company/sustainability/climate-strategy/climate-strategy.html

[26] Thyssenkrupp, “thyssenkrupp Steel is intensively pushing ahead with developing the hydrogen economy,” thyssenkrupp. Accessed: Feb. 24, 2024. [Online]. Available: https://www.thyssenkrupp.com/en/newsroom/press-releases/pressdetailpage/thyssenkrupp-steel-is-

intensively-pushing-ahead-with-developing-the-hydrogen-economy:-call-for-tenders-for-supplying-hydrogen-to-the-first-direct-reduction-plant-at-the-duisburg-location-251160

[27] F. Patisson and O. Mirgaux, “Hydrogen Ironmaking: How It Works,” *Metals*, vol. 10, no. 7, p. 922, Jul. 2020, doi: 10.3390/met10070922.

[28] M. Abdul Quader, S. Ahmed, S. Z. Dawal, and Y. Nukman, “Present needs, recent progress and future trends of energy-efficient Ultra-Low Carbon Dioxide (CO) Steelmaking (ULCOS) program,” *Renewable and Sustainable Energy Reviews*, vol. 55, pp. 537–549, Mar. 2016, doi: 10.1016/j.rser.2015.10.101.

[29] L. Chupa, P. E. Duarte, and HYL Technology Division, “The Importance of Iron Ores in Direct Reduction,” presented at the CVRD Seminar, Brazil, Sep. 2001.

[30] L. Yi, Z. Huang, T. Jiang, L. Wang, and T. Qi, “Swelling behavior of iron ore pellet reduced by H2–CO mixtures,” *Powder Technology*, vol. 269, pp. 290–295, Jan. 2015, doi: 10.1016/j.powtec.2014.09.018.

[31] A. Basdağ and A. Arol, “Coating of iron oxide pellets for direct reduction,” *Scandinavian Journal of Metallurgy*, vol. 31, pp. 229–233, Jul. 2002, doi: 10.1034/j.1600-0692.2002.310310.x.

[32] L. Yi, Z. Huang, T. Li, and T. Jiang, “Sticking of iron ore pellets in direct reduction with hydrogen and carbon monoxide: Behavior and prevention,” *Journal of Central South University*, vol. 21, Feb. 2014, doi: 10.1007/s11771-014-1968-6.

[33] L. Yi, Z. Huang, and T. Jiang, “Sticking of iron ore pellets during reduction with hydrogen and carbon monoxide mixtures: Behavior and mechanism,” *Powder Technology*, vol. 235, pp. 1001–1007, Feb. 2013, doi: 10.1016/j.powtec.2012.11.043.

[34] A. Bhaskar, M. Assadi, and H. Nikpey Somehsaraei, “Decarbonization of the Iron and Steel Industry with Direct Reduction of Iron Ore with Green Hydrogen,” *Energies*, vol. 13, no. 3, p. 758, Feb. 2020, doi: 10.3390/en13030758.

[35] L. Lorraine and V. Chevrier, “Direct from Midrex,” 2019.

[36] H. Ahmed, T. K. Sandeep Kumar, J. Alatalo, and B. Björkman, “Effect of carbon concentration and carbon bonding type on the melting characteristics of hydrogen-reduced iron ore pellets,” *Journal of Materials Research and Technology*, vol. 21, pp. 1760–1769, Nov. 2022, doi: 10.1016/j.jmrt.2022.10.019.

[37] A. Zakeri, K. S. Coley, and L. Tafaghodi, “Hydrogen-Based Direct Reduction of Iron Oxides: A Review on the Influence of Impurities,” *Sustainability*, vol. 15, no. 17, Aug. 2023, doi: 10.3390/su151713047.

[38] “Maximizing Iron Unit Yield from Ore to Liquid Steel (Part 1 - Ore Selection),” Midrex Technologies, Inc. Accessed: Feb. 19, 2024. [Online].

Available: https://www.midrex.com/tech-article/maximizing-iron-unit-yield-from-ore-to-liquid-steel-part-1-ore-selection/

[39] C. Barrington, "OBMS & Carbon Neutral Steelmaking. Whitepaper 3: Future DRI Production & Iron Ore Supply," IIMA, May 2022.

[40] "Adapting to raw materials challenges: Part 1 - Operating MIDREX plants with lower grade pellets & lump ores," Midrex Technologies, Inc. Accessed: Feb. 27, 2024. [Online]. Available: https://www.midrex.com/tech-article/adapting-to-raw-materials-challenges-part-1-operating-midrex-plants-with-lower-grade-pellets-lump-ores/

[41] S. Nicholas and S. Basirat, "Iron ore quality a potential headwind to green steelmaking," IEEFA, Jun. 2022.

[42] P. Cavaliere, *Hydrogen assisted direct reduction of iron oxides*. Cham: Springer, 2022.

[43] W. Liu, H. Zuo, J. Wang, Q. Xue, B. Ren, and F. Yang, "The production and application of hydrogen in steel industry," *International Journal of Hydrogen Energy*, vol. 46, no. 17, Mar. 2021, doi: 10.1016/j.ijhydene.2020.12.123.

[44] A. Nechache and S. Hody, "Alternative and innovative solid oxide electrolysis cell materials: A short review," *Renewable and Sustainable Energy Reviews*, vol. 149, p. 111322, Oct. 2021, doi: 10.1016/j.rser.2021.111322.

[45] O. Schmidt, A. Gambhir, I. Staffell, A. Hawkes, J. Nelson, and S. Few, "Future cost and performance of water electrolysis: An expert elicitation study," *International Journal of Hydrogen Energy*, vol. 42, no. 52, pp. 30470–30492, Dec. 2017, doi: 10.1016/j.ijhydene.2017.10.045.

[46] Tukes, "Vedyn käsittelyn ja varastoinnin turvallisuus," Jan. 2024. Accessed: Feb. 02, 2024. [Online]. Available: https://tukes.fi/vedyn-kasittelyn-ja-varastoinnin-turvallisuus

[47] B. Rego De Vasconcelos and J.-M. Lavoie, "Recent advances in power-to-x technology for the production of fuels and chemicals," *Front. Chem.*, vol. 7, p. 392, Jun. 2019, doi: 10.3389/fchem.2019.00392.

[48] M. Ji and J. Wang, "Review and comparison of various hydrogen production methods based on costs and life cycle impact assessment indicators," *International Journal of Hydrogen Energy*, vol. 46, no. 78, pp. 38612–38635, Nov. 2021, doi: 10.1016/j.ijhydene.2021.09.142.

[49] F. Dawood, M. Anda, and G. M. Shafiullah, "Hydrogen production for energy: An overview," *International Journal of Hydrogen Energy*, vol. 45, no. 7, pp. 3847–3869, Feb. 2020, doi: 10.1016/j.ijhydene.2019.12.059.

[50] Thyssenkrupp nucera, "Large-scale water electrolysis for green hydrogen production," 2022. [Online]. Available: https://thyssenkrupp-

nucera.com/wp-content/uploads/2022/11/thyssenkrupp-nucera-green-hydrogen-solutions-brochure.pdf

[51] C. Boehm *et al.*, "MIDREX H2 — The road to co2-free iron and steelmaking," in *AISTech 2021 Proceedings of the Iron and Steel Technology Conference*, AIST, 2021, pp. 262–273. doi: 10.33313/382/025.

[52] R. B. Gupta, A. Basile, and T. N. Veziroğlu, Eds., *Compendium of hydrogen energy. Volume 2: Hydrogen storage, distribution and infratructure / edited by Ram B. Gupta, Angelo Basile, T. Nejat Veziroğlu*. in Woodhead Publishing series in energy, no. number 84. Amsterdam Boston Cambridge Heidelberg: Elsevier, WP Woodhead Publishing, 2016.

[53] J. Ekhebume Ogbezode, O. Olufemi Ajide, O. Olugbemiga Oluwole, and O. Ofi, "Recent trends in the technologies of the direct reduction and smelting process of iron ore/iron oxide in the extraction of iron and steelmaking," in *Iron Ores and Iron Oxides - New Perspectives*, B. Kumar, Ed., IntechOpen, 2023. doi: 10.5772/intechopen.1001158.

[54] K. Huitu, M. Kekkonen, and L. Holappa, "Novel steelmaking processes – Literature study and critical review," Nov. 2009.

[55] O. Milling, C. Atkinson, and M. Allan, "H2DRI Pilot project public report," Materials Processing Institute, Feb. 2023.

[56] "The versatile OBM (ore-based metallic): part 2 - how to get what you paid for: a guide to maintaining the value of DRI," Midrex Technologies, Inc. Accessed: Feb. 28, 2024. [Online]. Available: https://www.midrex.com/tech-article/the-versatile-obm-ore-based-metallic-part-2-how-to-get-what-you-paid-for-a-guide-to-maintaining-the-value-of-dri/

[57] Midrex, "2022 World Direct Reduction Statistics," Midrex, Dec. 2023. Accessed: Jan. 23, 2024. [Online]. Available: https://www.midrex.com/wp-content/uploads/MidrexSTATSBook2022.pdf

[58] A. Baroyan, O. Kravchenko, C. Prates, S. Vercammen, and B. Zeumer, "The resilience of steel: Navigating the crossroads | McKinsey." Accessed: Jan. 30, 2024. [Online]. Available: https://www.mckinsey.com/industries/metals-and-mining/our-insights/the-resilience-of-steel-navigating-the-crossroads

[59] V. Chevrier, "MIDREX Flex™: Minimizing technology risks in the transition to carbon-free steelmaking," WSA Breakthrough Technology Conference, Dec. 06, 2023.

[60] K. Huitu, M. Helle, H. Helle, M. Kekkonen, and H. Saxén, "Optimization of Midrex Direct Reduced Iron Use in Ore-Based Steelmaking," *steel research int.*, vol. 86, no. 5, pp. 456–465, May 2015, doi: 10.1002/srin.201400091.

[61] R. Gyllenram, W. Friesinger, and C. Boehm, "Direct Reduced Iron Webinar," May 23, 2024.

[62] B. Hou, H. Zhang, H. Li, and Q. Zhu, “Study on Kinetics of Iron Oxide Reduction by Hydrogen,” *Chinese Journal of Chemical Engineering*, vol. 20, no. 1, pp. 10–17, Feb. 2012, doi: 10.1016/S1004-9541(12)60357-7.

[63] D. Spreitzer and J. Schenk, “Reduction of Iron Oxides with Hydrogen—A Review,” *steel research int.*, vol. 90, no. 10, p. 1900108, Oct. 2019, doi: 10.1002/srin.201900108.

[64] “FactSage.com.” Accessed: Mar. 19, 2024. [Online]. Available: https://www.factsage.com/

[65] K. Jabbour and N. El Hassan, “Optimized conditions for reduction of iron (III) oxide into metallic form under hydrogen atmosphere: A thermodynamic approach,” *Chemical Engineering Science*, vol. 252, p. 117297, Apr. 2022, doi: 10.1016/j.ces.2021.117297.

[66] “Electrical Heating of MIDREX® Process Gases,” Midrex Technologies, Inc. Accessed: May 29, 2024. [Online]. Available: https://www.midrex.com/tech-article/electrical-heating-of-midrex-process-gases/

[67] M. Bailera, P. Lisbona, B. Peña, and L. M. Romeo, “A review on CO2 mitigation in the Iron and Steel industry through Power to X processes,” *Journal of CO2 Utilization*, vol. 46, p. 101456, Apr. 2021, doi: 10.1016/j.jcou.2021.101456.

[68] R. Sah and S. Dutta, “Direct Reduced Iron: Production,” 2016, p. pp 1082-1108. doi: 10.1081/E-EISA-120050996.

[69] H. Hamadeh, O. Mirgaux, and F. Patisson, “Detailed Modeling of the Direct Reduction of Iron Ore in a Shaft Furnace,” MATERIALS SCIENCE, preprint, Sep. 2018. doi: 10.20944/preprints201809.0115.v1.

[70] A. Ghosh and A. Chatterjee, *Ironmaking and steelmaking: theory and practice*, 3. print. in Eastern economy edition. New Delhi: PHI Learning, 2010.

[71] M. G. K. Grant, Ph. Blostein, S. But, and C. Kaufman, “Adaptation of EAF Operations for Unconventional Raw Materials,” *Metallurgist*, vol. 58, no. 1–2, pp. 95–104, May 2014, doi: 10.1007/s11015-014-9875-5.

[72] R. Gyllenram, N. Arzpeyma, W. Wei, and P. G. Jönsson, “Driving investments in ore beneficiation and scrap upgrading to meet an increased demand from the direct reduction-EAF route,” *Miner Econ*, vol. 35, no. 2, pp. 203–220, Jun. 2022, doi: 10.1007/s13563-021-00267-2.

[73] M. S. A. Elkader, A. M. Fathy, M. Eissa, and S. A. Shama, “Effect of Direct Reduced Iron Proportion in Metallic Charge on Technological Parameters of EAF Steelmaking Process,” 2016. [Online]. Available: https://api.semanticscholar.org/CorpusID:53345463

[74] E-mail conversation with Mohamed Abd-Elkader, Ezz Steel, Mar. 21, 2024.

[75] M. Kirschen, K. Badr, and H. Pfeifer, “Influence of direct reduced iron on the energy balance of the electric arc furnace in steel industry,” *Energy*, vol. 36, no. 10, pp. 6146–6155, Oct. 2011, doi: 10.1016/j.energy.2011.07.050.

[76] “EU-27 Steel scrap spesification” Accessed: Mar. 19, 2024. [Online]. Available: https://www.mgg-recycling.com/wp-content/uploads/2013/06/EFR_EU27_steel_scrap_specification.pdf

[77] S. Durowaye, “Effect of Copper on Microstructure and Mechanical Properties of Construction Steel,” *World Academy of Science, Engineering and Technology International Journal of Chemical, Nuclear, Metallurgical and Materials Engineering*, vol. 8, pp. 785–789, Jan. 2014.

[78] K. E. Daehn, A. C. Serrenho, and J. Allwood, “Finding the Most Efficient Way to Remove Residual Copper from Steel Scrap,” *Metall Mater Trans B*, vol. 50, no. 3, pp. 1225–1240, Jun. 2019, doi: 10.1007/s11663-019-01537-9.

[79] V.-V. Visuri, “The future of scrap supply,” presented at the WCEF2023 Accelerator Session: The Role of Scrap in Steel Sector Decarbonization, Jun. 01, 2023.

[80] P. Duarte, “Trends in H2-based steelmaking,” *Steel Times International*, Feb. 2019.

[81] T. Echterhof, “Review on the Use of Alternative Carbon Sources in EAF Steelmaking,” *Metals*, vol. 11, no. 2, p. 222, Jan. 2021, doi: 10.3390/met11020222.

[82] A. Fontana, P. O’kane, D. O’Connell, V. Sahajwalla, and M. Zaharia, “Injection of recycled tyres in EAF steelmaking as a slag foaming agent,” *Steel Times International*, vol. 36, no. 6, pp. 17-18,20, Sep. 2012.

[83] L. Kieush and J. Schenk, “Investigation of the Impact of Biochar Application on Foaming Slags with Varied Compositions in Electric Arc Furnace-Based Steel Production,” *Energies*, vol. 16, no. 17, p. 6325, Aug. 2023, doi: 10.3390/en16176325.

[84] A. Vickerfält, “A study of an autogenous slag for steel production with consideration of possible vanadium extraction,” Doctoral Thesis, KTH Royal Institute of Technology, Stockholm, Sweden, 2024. Accessed: Feb. 21, 2024. [Online]. Available: https://kth.diva-portal.org/smash/record.jsf?pid=diva2%3A1836313&dswid=199

[85] J. H. Heo and J. H. Park, “Effect of Direct Reduced Iron (DRI) on Dephosphorization of Molten Steel by Electric Arc Furnace Slag,” *Metall Mater Trans B*, vol. 49, no. 6, pp. 3381–3389, Dec. 2018, doi: 10.1007/s11663-018-1406-5.

[86] M. Kirschen, T. Hay, and T. Echterhof, “Process Improvements for Direct Reduced Iron Melting in the Electric Arc Furnace with Emphasis on

Slag Operation," *Processes*, vol. 9, no. 2, p. 402, Feb. 2021, doi: 10.3390/pr9020402.

[87] S. Manocha and F. Ponchon, "Management of Lime in Steel," *Metals*, vol. 8, no. 9, p. 686, Aug. 2018, doi: 10.3390/met8090686.

[88] S. Hornby, J. Madias, and F. Torre, "Myths and Realities of Charging DRI/HBI in Electric Arc Furnaces," *Iron and Steel Technology*, vol. 13, p. 81, Mar. 2016.

[89] D. Nuber, H. Eichberger, and B. Rollinger, "Circored fine ore direct reduction - The future of modern electric steelmaking," *Millennium Steel 2006*, vol. 126, pp. 47–51, Mar. 2006.

[90] S. Hornby, "Hydrogen-Based DRI EAF Steelmaking — Fact or Fiction?," Jan. 2021, p. 261. doi: 10.33313/382/124-20513-048.

[91] "DevH2forEAF project." Accessed: May 20, 2024. [Online]. Available: https://www.rina.org/en/media/CaseStudies/DevH2forEAF

[92] L. Schüttensack, A. Reinicke, and T. Echterhof, "Application of hydrogen operated burners in the electric arc furnace," presented at the 5th European Academic Symposium on EAF Steelmaking,

[93] T. Echterhof, "Sustainable EAF steelmaking," Steeluniversity, RWTH Aachen University, Sep. 21, 2023.

[94] V. Vogl, M. Åhman, and L. J. Nilsson, "Assessment of hydrogen direct reduction for fossil-free steelmaking," *Journal of Cleaner Production*, vol. 203, pp. 736–745, Dec. 2018, doi: 10.1016/j.jclepro.2018.08.279.

[95] J. Andersson, "Non-geological hydrogen storage for fossil-free steelmaking," PhD Thesis, 2022.

[96] P. Stagnoli, Director of Sales and Marketing at Tenova, "H2 based DRI: The safe solution to decarbonize the iron and steel industry," Accessed: Feb. 04, 2024. [Online]. Available: https://www.youtube.com/watch?v=puBi3hzzBtk

[97] B. N. Liu, Q. Li, Z. S. Zou, and A. B. Yu, "Discussion on chemical energy utilisation of reducing gas in reduction shaft furnace," *Ironmaking & Steelmaking*, vol. 41, no. 8, pp. 568–574, Sep. 2014, doi: 10.1179/1743281213Y.0000000168.

[98] "HOTLINK® SYSTEM BENEFITS OF CHARGING HOT DRI (HDRI)," Midrex Technologies, 2014.

[99] R. L. González *et al.*, "Improvements in yield in an all-DRI-fed EAF from minimization of FeO generation during melting as well as post-reduction of FeO from residual slag," *Iron and Steel Technology*, vol. 15, pp. 36–41, Jan. 2018.

[100] M. Kirschen, "Visualization of Slag Data for Efficient Monitoring and Improvement of Steelmaking Slag Operation in Electric Arc Furnaces,

with a Focus on MgO Saturation," *Metals*, vol. 11, no. 1, p. 17, Dec. 2020, doi: 10.3390/met11010017.

[101] N. Arzpeyma, R. Gyllenram, and P. G. Jönsson, "Development of a Mass and Energy Balance Model and Its Application for HBI Charged EAFs," *Metals*, vol. 10, no. 3, p. 311, Feb. 2020, doi: 10.3390/met10030311.

[102] I. Ekmekci, Y. Yetişken, and U. Camdali, "Mass Balance Modeling for Electric Arc Furnace and Ladle Furnace System in Steelmaking Facility in Turkey," *Journal of Iron and Steel Research International - J IRON STEEL RES INT*, vol. 14, Sep. 2007, doi: 10.1016/S1006-706X(07)60064-8.

[103] L. Ferro, P. Giugliano, P. Galbiati, F. Memoli, C. Giavani, and J. Maiolo, "The Electric Arc Furnace of Tenaris Dalmine: from the application of the new technologies of digital electrode regulation and multipoint injection to the Dynamic Control of the Process," presented at the 16th IAS Steelmaking Conference, Rosaria, Argentina, 2007, pp. 59–72.

[104] I. Hassan, K. G.I., S. E, and G. Megahed, "phosphorous behavior in electric arc furnace steelmaking with the melting of high phosphorous content direct reduced iron," Jun. 2015.

[105] N. Müller, G. Herz, E. Reichelt, M. Jahn, and A. Michaelis, "Assessment of fossil-free steelmaking based on direct reduction applying high-temperature electrolysis," *Cleaner Engineering and Technology*, vol. 4, p. 100158, Oct. 2021, doi: 10.1016/j.clet.2021.100158.

[106] G. Gavaliere, "Analysis on copper, lead and tin removal in steel scrap sorting," Master's Thesis, KTH Royal Institute of Technology, 2023.

[107] J. Jones, "The Role of Steel Scrap in Decarbonization," presented at the WorldSteel Climate Action Open Forum, Dec. 09, 2023.

[108] M. Fischedick, J. Marzinkowski, P. Winzer, and M. Weigel, "Techno-economic evaluation of innovative steel production technologies," *Journal of Cleaner Production*, vol. 84, pp. 563–580, Dec. 2014, doi: 10.1016/j.jclepro.2014.05.063.

[109] S. Ollila and T. Paananen, "Activities regarding transformation to fossil free steel making at SSAB Raahe," Nordic sustainability day, University of Oulu, Feb. 01, 2023.

[110] B. Monsen, E. Thomassen, I. Brakstad, E. Ringdalen, and P. H. Hoegaas, "Characterization of DR Pellets for DRI Applications," May 2015.

[111] S. Bell, B. Davis, A. Javaid, and E. Essadiqi, "Final Report on Refining Technologies of Steel," 2006, doi: 10.13140/RG.2.2.30591.41120.

[112] "Atmospheric Alkaline Electrolyser," Nel Hydrogen. Accessed: May 07, 2024. [Online]. Available: https://nelhydrogen.com/product/atmospheric-alkaline-electrolyser-a-series/

[113] L. Shao, X. Zhang, C. Zhao, Y. Qu, H. Saxén, and Z. Zou, "Computational analysis of hydrogen reduction of iron oxide pellets in a shaft furnace

process," *Renewable Energy*, vol. 179, pp. 1537–1547, Dec. 2021, doi: 10.1016/j.renene.2021.07.108.

[114] U. Lubenau, H. Bültemeier, C. Marrune, J. Hüttenrauch, and P. Pietsch, "H2 short study: Hydrogen quality in an overall German hydrogen network," DBI Gas- und Umwelttechnik GmbH, Jun. 2022.

[115] T. Hay, V.-V. Visuri, M. Aula, and T. Echterhof, "A Review of Mathematical Process Models for the Electric Arc Furnace Process," *steel research int.*, vol. 92, no. 3, p. 2000395, Mar. 2021, doi: 10.1002/srin.202000395.

[116] A. G. Belkovskii, S. F. Filippov, and Ya. L. Kats, "Optimum content of carbon in the charge of an EAF," *Metallurgist*, vol. 56, no. 11–12, pp. 810–818, Mar. 2013, doi: 10.1007/s11015-013-9656-6.

[117] A. Pesamosca and D. Patrizio, "Latest trends in EAF optimization of scrapbased melting process: balancing chemical and electrical energy input for competitive and sustainable steelmaking," Sep. 2017, pp. 169–182. doi: 10.5151/1982-9345-27626.

[118] M. Korpyś, J. Wójcik, and P. Synowiec, "Methods for sweetening natural and shale gas," *Chemik Science-Technique-Market*, vol. 68, pp. 213–215, Mar. 2014.

[119] B. Diaconu, L. Anghelescu, and M. Cruceru, "Analysis of energy balance for a steel Electric Arc Furnace," *WSEAS TRANSACTIONS ON ENVIRONMENT AND DEVELOPMENT*, vol. 16, pp. 48–56, Mar. 2020, doi: 10.37394/232015.2020.16.6.

[120] R. KÜHN, H. GECK, and K. SCHWERDTFEGER, "Continuous off-gas measurement and energy balance in Electric Arc Steelmaking," *Isij International - ISIJ INT*, vol. 45, pp. 1587–1596, Jan. 2005, doi: 10.2355/isijinternational.45.1587.

[121] A. Laukka and P. Palovaara, "Discussions with Aleksi Laukka and Petri Palovaara from AFRY," 2024.

[122] H. Pfeifer and M. Kirschen, "Thermodynamic analysis of EAF electrical energy demand," in *8th European Electric Steelmaking Conference*, May 2002.

Appendix A. General assumptions in the model

Some of the most important assumptions made for the simulation flowsheet are listed below:

1. All material properties (e.g. Enthalpies and heat capacities) are from the HSC databases, unless otherwise specified.
2. All calculations are done to produce 1 ton of liquid steel that exits the EAF. This is controlled in the simulation flowsheet.
3. The results (energy consumption, slag and the end-product etc.) does not consider the stages of ore mining, pelletizing, beneficiation or further steel refining/finishing steps.
4. The values used in the model have been collected from available literature, industry benchmarks and comments from supervisors, the sources have been stated as clearly as possible. No laboratory or pilot-scale experimental work has been completed in this research.

Appendix B. Assumed iron ore pellet composition for HSC

Table 1. The chemical composition of the examined pellet grades [11], [36], [40] and [110].

Component	**Case 1: Bf-Grade IO pellet, Wt.%**	**Case 2: DR-Grade IO pellet, Wt.%**	**Case 3: High quality DR-Grade IO pellet, Wt.%**
Tot. Fe	63.9	67.1	68.2
Tot. gangue	8.5	4.0	2.5
Fe_2O_3	91.4	95.9	97.5
SiO_2	3.66	1.50	0.94
CaO	2.30	1.01	0.63
MgO	1.02	0.51	0.32
Al_2O_3	0.43	0.41	0.26
V_2O_5	0.38	0.19	0.12
TiO_2	0.34	0.18	0.11
MnO	0.21	0.10	0.06
Na_2O	0.051	0.032	0.020
K_2O	0.051	0.024	0.015
P_2O_5	0.117	0.082	0.052
FeS	0.047	0.016	0.010

Appendix C. Assumed scrap composition for HSC

Table 2. The chemical composition of the steel scrap used in the model [11], [111].

Parameter	**Wt.%**
Fe (balance)	95.23
C	0.40
CaO	0.90
MgO	0.25
Al_2O_3	0.43
SiO_2	0.95
P	0.035
S	0.040
Mn	0.55
Zn	0.45
Si	0.25
Cu	0.25
Ni	0.090
Cr	0.15
Sn	0.013
Mo	0.02
Pb	0.03

Appendix D. Shaft furnace parameters for HSC

Table 3. Assumptions for the simulation of hydrogen heater, shaft furnace and transportation heat losses.

Parameter	Value	Unit	Comment	Source
The reducing gas temperature before heating	80	°C	A typical temperature from AEL.	[47], [48], [112]
The reducing gas temperature after heating	900	°C		[95], [113]
Electrical hydrogen heater efficiency	0.9	-	Energy consumption calculated based on supplied hydrogen.	[34], [66]
Hydrogen electrolysis energy consumption	4.5	kWh/Nm^3	Energy consumption calculated based on consumed hydrogen (rest can be circulated). Typical value for AEL rest can be circulated.	[47], [50]
Lambda ratio that represents the excess amount of hydrogen	3.5	-	Set in order to ensure proper heat balance and GOD-value.	
Hydrogen purity in the reducing gas	99.8	vol.%	Complies with ISO Grade A.	[51], [114]
Water amount in the reducing gas	0.13	vol.%	Assumed to contain two impurities with volume fraction 2:1 (H_2O:O_2).	
Oxygen amount in the reducing gas	0.07	vol.%		
Metallisation achieved (Case 1A, 1B, 1C)	93	%		[34], [40], [75], [95]
Metallisation achieved (Case 2A, 2B, 2C)	94	%		[34], [40], [75], [95]
Metallisation achieved (Case 3A, 3B, 3C)	94.75	%		[34], [40], [75], [95]
DRI exit temperature from the shaft furnace	725	°C	A lower value that with NG based process assumed.	[97]
Heat Losses in the shaft furnace	40	kWh/tls		[95]
DRI temperature after transportation	600	°C		[98]

Appendix E. Electric Arc Furnace Parameters for HSC

Table 4. Assumptions for the simulation of electric arc furnace.

Parameter	Value	Unit	Comment	Source
Graphite electrode consumption	3	kg/tls	Based on a typical mass balance for EAF.	[115]
Refractories consumption	3	kg/tls	Based on a typical mass balance for EAF.	[115]
Total carbon (Case 1A, 2A, 3A)	24	kg/tls	More carbon consumed vs. NG. based DRI. More carbon consumed when the ratio of DRI to scrap increases in the charge.	[73], [86], [116]
Total carbon (Case 1B, 2B, 3B)	18	kg/tls		[73], [86], [116]
Total carbon (Case 1C, 2C, 3C)	12	kg/tls		[73], [86], [116]
Basicity B2 target	2.1	-	Value cited in literature & realised in industrial EAFs.	[86], [104], [103]
Basicity B4 measured	-	-	B4 ranges from 2.03 to 2.30. Validated from industrial EAFs.	[86], [104], [103]
Slag former composition (given in wt.%)	85 12.5 1.25 1.25	%CaO %MgO %SiO_2 %Al_2O_3		[73], [87]
Infiltrated air	130	Nm^3/tls	Based on a typical mass balance for EAF.	[115]
Oxygen blowing	30	Nm^3/tls		[75], [117]
Natural gas (Case 1A, 2A, 3A)	1.7	Nm^3/tls	Based on typical EAF operation. More NG burners used when the ratio of scrap to DRI increases.	[73]
Natural gas (Case 1B, 2B, 3B)	2.3	Nm^3/tls		[73]
Natural gas (Case 1C, 2C, 3C)	4.0	Nm^3/tls		[73], [103], [117]
Natural gas composition (given in vol.%)	90.95 8.2 0.85	%CH_4 %C_2H_6 %C_3H_8	Typical composition.	[118]
Liquid steel temperature	1600	°C		[86], [119]
Slag temperature	1650	°C		[119]

Off gas temperature	1150	°C	Varies based on the melting stage typically from 900-1600 °C.	[120]
Heat Losses (Case 1A, 2A, 3A)	120	kWh/tls	Corresponds to approximately 30% of the energy consumption of the EAF. Longer tap-to-tap times leads to higher losses.	[121]
Heat Losses (Case 1B, 2B, 3B)	110	kWh/tls		[121]
Heat Losses (Case 1C, 2C, 3C)	100	kWh/tls		[121]
Efficiency	0.6	-	Typical efficiency of the arcs.	[75], [122]
Tap-to-tap time (Case 1A, 2A, 3A)	60	min	Based on typical EAF operation. The tap-to-tap time decreases when the ratio of scrap to DRI increases in the feed.	[73], [75], [88], [117],
Tap-to-tap time (Case 1B, 2B, 3B)	55	min		[73], [75], [88], [117],
Tap-to-tap time (Case 1C, 2C, 3C)	50	min		[73], [75], [88], [117],
Power on time	TTT-10	min	Tap-to-tap time minus 10 minutes, which is typical for industrial EAFs.	[75], [103], [117]

Appendix F. Elemental distribution in the EAF

Table 5. Elemental distributions used in the EAF modelling.

Element	Distribution & Rationale	Source
Al	Distribution ratio (%slag/%melt) set to 111.	[101]
Ar	Ar is only from the infiltrated air, thus 100% to off gas.	
C	Controlled so that 0.03 wt.% in the steel, rest balanced between dust (according to reference) and off gas.	[101]
Ca	100% to slag phase as CaO.	
Cr	Distribution ratio (%slag/%melt) set to 4.	[101], [104]
Cu	100% to metal phase.	[102]
Fe	HSC control used so that 30% to slag phase, rest balanced between dust (according to reference) and slag	[101]
H	100% to off gas so that a little amount of water vapour is formed.	
K	100% to slag phase as K_2O.	
Mg	100% to slag phase as MgO.	
Mn	Distribution ratio (%slag/%melt) set to 24.	[101]
Mo	100% to liquid steel.	[101]
N	N is only from the infiltrated air, thus 100% to off gas.	
Na	100% to slag phase as Na_2O.	
Ni	Assumed 95% to metal, rest to slag as NiO.	[104]
O	Balanced to the compounds present in the system. Rest to off gas as O_2.	
P	65% of the metallic phosphorus to slag. All oxides to the slag phase	[102], [104],
Pb	Very little amount present in the system, 100% to dust.	[101]
S	Elemental S to metallic phase, and sulfur from DRI to slag phase, balance amount to dust.	[101], [104]
Si	90% of metallic Si to slag, rest to metal. All oxides to the slag phase.	[101], [102]
Sn	100% to metal phase (assumed similar behaviour as copper).	
Ti	Distribution ratio (%slag/%melt) set to 453.	[101]
V	100% to slag phase as V_2O_5, only originates from the DRI.	[101]
Zn	100% to dust phase.	[101]

Appendix G. Results from the model

	Case 1A	Case 2A	Case 3A	Case 1B	Case 2B	Case 3B	Case 1C	Case 2C	Case 3C
Shaft Furnace:									
HDRI production, kg/tls	972	897	869	579	534	518	221	204	198
HDRI temperature, °C	725	725	725	725	725	725	725	725	725
Pellet consumption, kg/tls	1316	1241	1212	784	739	722	300	282	276
Metallisation, %	93.0	94.0	94.75	93.0	94.0	94.75	93.0	94.0	94.75
Hydrogen consumption, Nm^3/tls	1725	1718	1714	1027	1024	1021	393	391	390
Vapour production, Nm^3/tls	1724	1717	1712	1027	1023	1020	392	391	390
Vapour temperature, °C	309	331	338	268	289	297	101	122	129
Electric Arc Furnace:									
Total C consumption, kg/tls	24.0	24.0	24.0	18.0	18.0	18.0	12.0	12.0	12.0
Oxygen consumption, Nm^3/tls	30.0	30.0	30.0	30.0	30.0	30.0	30.0	30.0	30.0
Burner consumption, Nm^3/tls	1.7	1.7	1.7	2.3	2.3	2.3	4	4	4
Electrode consumption, kg/tls	3	3	3	3	3	3	3	3	3
Refractory consumption, kg/tls	3	3	3	3	3	3	3	3	3
Slag former mass, kg/tls	90	35	22	64	31	23	40	27	24
Basicity (B2), -	2.10	2.10	2.10	2.10	2.10	2.10	2.10	2.10	2.10
Basicity (B4), -	2.30	2.11	2.14	2.24	2.07	2.08	2.14	2.03	2.03
Scrap Consumption, kg/tls	242.9	211.3	207.0	578.8	560.0	557.4	884.5	877.4	876.4
Tapped Slag, kg/tls	304	134	88	220	119	91	143	105	95
Slag Temperature, °C	1650	1650	1650	1650	1650	1650	1650	1650	1650
Produced Off-Gas, Nm^3/tls	175	181	182	179	183	183	196	197	198
Off-Gas Temperature, °C	1150	1150	1150	1150	1150	1150	1150	1150	1150
Produced CO_2, kg/tls	104.5	104.0	103.9	88.7	88.4	88.4	74.8	74.7	74.7
Produced Dust, kg/tls	9.5	9.2	9.2	12.2	12.0	12.0	14.7	14.6	14.6

Energy Consumption:									
Hydrogen preheating, kWh/tls	857	854	852	511	509	507	195	194	194
Preheating efficiency, -	0.9	0.9	0.9	0.9	0.9	0.9	0.9	0.9	0.9
Electric Arc Furnace, kWh/tls	509	446	421	450	417	403	392	381	376
Steel:									
Tapped Steel, kg/tls	1000.0	1000.0	1000.0	1000.0	1000.0	1000.0	1000.0	1000.0	1000.0
Tapped Steel Temperature, °C	1600	1600	1600	1600	1600	1600	1600	1600	1600
Fe, wt.%	99.84	99.86	99.86	99.68	99.69	99.69	99.53	99.54	99.54
C, ppm	300	300	300	300	300	300	300	300	300
Mn, ppm	130	75	59	168	135	126	203	191	187
P, ppm	30	26	25	71	69	68	108	107	107
S, ppm	97	87	85	231	222	219	354	319	313
Si, ppm	61	50	53	145	136	140	227	221	215
Cr, ppm	61	53	52	163	157	157	255	252	252
Al, ppm	37	31	21	32	28	22	27	25	23
Cu, ppm	607	528	517	1447	1400	1393	2211	2194	2191
Ni, ppm	208	181	177	495	479	477	756	750	749
Ti, ppm	6	3	2	4	2	1	1	1	0
Mo, ppm	43	37	36	101	98	98	155	154	153
Sn, ppm	30	26	26	72	70	70	111	110	110
Residuals (Cu, Ni, Sn, Mo), ppm	888	772	757	2115	2048	2037	3233	3207	3203